A review of Titan's atmospheric phenomena

Mathieu Hirtzig, Tetsuya Tokano, Sébastien Rodriguez, Stéphane Le Mouélic, Christophe Sotin

Astron Astrophys Rev
DOI 10.1007/s00159-009-0018-0

REVIEW ARTICLE

A review of Titan's atmospheric phenomena

Mathieu Hirtzig · Tetsuya Tokano · Sébastien Rodriguez · Stéphane le Mouélic · Christophe Sotin

Received: 24 December 2008 / Revised: 17 February 2009

Abstract Saturn's satellite Titan is a particularly interesting body in our solar system. It is the only satellite with a dense atmosphere, which is primarily made of nitrogen and methane. It harbours an intricate photochemistry, that populates the atmosphere with aerosols, but that should deplete irreversibly the methane. The observation that methane is not depleted led to the study of Titan's methane cycle, starting with its atmospheric part. The features that inhabit Titan's atmosphere can last for timescales varying from year to day. For instance, the reversal of the north–south asymmetry is linked to the 16-year seasonal cycle. Diurnal phenomena have also been observed, like a stratospheric haze enhancement or a possible tropospheric drizzle. Furthermore, clouds have been reported on Titan since 1993. From these first detections and up to now, with the recent inputs from the Cassini–Huygens mission, clouds have displayed a large range of shapes, altitudes, and natures, from the flocky tropospheric clouds at the south pole to the stratiform ones in the northern stratosphere. It is still difficult to compose a clear picture of the physical processes governing these phenomena, even

M. Hirtzig (✉)
LATMOS, IPSL, Verrières-le-Buisson, France
e-mail: mathieu.hirtzig@aerov.jussieu.fr

T. Tokano
Institut für Geophysik und Meteorologie, Universität zu Köln, Cologne, Germany

S. Rodriguez
Laboratoire AIM, CEA/DSM, CNRS, Université Paris Diderot, IRFU/SAp,
Gif-sur-Yvette, France

S. le Mouélic
Laboratoire de Planétologie et Géodynamique, Nantes, France

C. Sotin
Jet Propulsion Laboratory, Pasadena, CA, USA

Published online: 20 March 2009

though of lot of different means of observation (spectroscopy, imaging) are available now. We propose here an overview of the phenomena reported between 1993 and 2008 in the low atmosphere of Titan, with indications on the location, altitude, and their characteristics in order to give a perspective of our up-to-date understanding of Titan's meteorological manifestations. We shall focus mainly on direct imaging observations, from both space- and ground-based facilities. All of these observations, published in more than 30 different refereed papers to date, allow us to build a precise chronology of Titan's atmospheric changes (including the north–south asymmetry, diurnal and seasonal effects, etc). Since the interpretation is at an early stage, we only briefly mention some of the current theories regarding the features' nature.

Keywords Titan, satellites · Near-infrared · Clouds · Imagery, spectroscopy, spectro-imagery

1 Introduction

Although several spacecraft—Pioneer, Voyager 1, 2, and Cassini/Huygens—have visited the Kronian system, complementing a century of ground-based observations, astronomers still struggle to fully understand the intricate dynamics of Titan's atmosphere. The images of Voyager taken in the visible showed a clear asymmetry between the southern and northern hemispheres (Smith et al. 1982), and a detached layer of haze above 400 km (Rages and Pollack 1983). Flasar et al. (1981) and Lindal et al. (1983) described the vertical structure and the temperature profile of the atmosphere, as well as its chemical composition. Sromovsky et al. (1981) first hinted the seasonal periodicity of the north–south asymmetry, and Sagan and Thompson (1982) focused on the chemistry of Titan's organic aerosols. Eventually, McKay et al. (1989) reproduced the thermal structure of the atmosphere with a radiative–convective model including for the first time the aerosols microphysics. At this epoch, the consumption of methane was well known, but there was no clear evidence for a methane cycle.

Until the beginning of the 1990s, no firm detection of clouds on Titan was made. As the collision-induced absorptions of tropospheric gases could not solely explain the continuum observed in infrared spectra of Voyager 1/IRIS, Courtin (1982) and Samuelson (1983) suggested that methane clouds could explain the remainder. Clouds were also hypothesized as one possible mechanism to explain the scintillation of the Voyager 1 radio-occultation profile (Lindal et al. 1983; Hinson 1983). Toon et al. (1988) suggested that methane clouds probably existed from altitudes below 10 km up to about 30 km, that the optical depth of these clouds would be typically of the order of 2–5 in both the infrared and the visible, and that such clouds would be patchy. The uncertainty of the interpretation of the Voyager infrared data was partly due to uncertain collision-induced absorption coefficients. When updated absorption coefficients became available in the 1990s, Courtin et al. (1995) and Samuelson et al. (1997b) found evidence of large methane supersaturation in the mid-troposphere. If this were the case, it would contradict the presence of a permanent cloud deck or the occurrence of moist convection.

However, from spectra taken in 1993 and 1995, Griffith et al. (1998) discovered the presence of reflective layers, or clouds, in Titan's atmosphere. Since then and for more than a decade now, clouds and other atmospheric phenomena have been reported on Titan by various investigators. We now know that many transient features inhabit Titan's atmosphere, but in most cases we lack specific information, such as altitude range, density, frequency, chemical composition, or particle size distribution, that would enable us to get a full picture of Titan's meteorology. Our purpose here is to build an extensive report of the observations of cloud features and other atmospheric phenomena, as well as a timeline of such detections, between 1993 and 2008. Reviews addressing Titan's meteorology dynamics can be found in Hunten et al. (1984), Flasar (1998a,b), Flasar and Achterberg (2008), and Tokano (2008b). Hereafter, we first briefly summarize the techniques used for these observations, then enumerate the various cloud reports through more than a decade worth of publications. We include other long-term atmospheric phenomena that may influence the detectability of clouds such as the north–south seasonal asymmetry. We finally indicate the various interpretations given for each phenomenon. Our first goal is to build a full timeline of all the meteorological phenomena. As a second goal, we try to establish if all the diverse phenomena reported up to now ("transient clouds", "zonal streaks", "polar clouds system", "polar collars" and so on) may or may not be facets of the same phenomena. Indeed, techniques, observations, denominations, and interpretations are so varied that it is probable that some of these different names correspond in fact to the same type of clouds. We will show that it is plausible to distinguish two main types of Titan's clouds inhabiting either the troposphere or the stratosphere. We finally compare our results to current cloud models and show how their presence and evolution through the atmosphere can be predicted by such models.

2 Observational tools applied to Titan

Various means can be used to observe Titan's atmospheric processes. We do not intend to give a full description of each, but briefly refer to the different techniques and processing methods used in cloud-reporting articles, where the reader can find more detailed technical information. Depending on the instrument, the technique, and the model used, the interpretation can vary significantly. This led us to consider observations and interpretations separately hereafter.

2.1 Observational techniques from the ground

To analyse Titan's clouds, some parameters are crucial: spatial resolution, spectral resolution, and wavelength range. Sharp spatial resolution allows us to resolve, localise, and monitor the clouds. High spectral resolution allows us to retrieve—via a model—the altitude of these clouds, and infer hints regarding the properties of their particles (composition, size, distribution, and so on). From the Earth, Titan's diameter (0.8 arcsec) is usually smaller than the seeing (the atmospheric turbulence which blurs the sharp details smaller than 1 arcsec). To resolve features on Titan's disk, we need to minimise or avoid Earth's atmospheric turbulence. Three options are available:

moving to space (HST), freezing its effects (speckle imagery), or correcting them (adaptive optics).

2.1.1 Full-disk spectroscopy

Full-disk spectroscopy of Titan has been in use regularly for nearly two decades now. All the light from the target is focused on a slit and dispersed via a grating system to recover a high signal-to-noise ratioed spectrum. But such a method forbids the resolution of features on Titan's disk (since it is smaller than the slit width), even though the presence of clouds can be detected if they are bright enough to modify the averaged spectrum. The very first spectrum of Titan was acquired at the McDonald Observatory by Kuiper (1944), detecting the presence of atmospheric methane.[1] The first exploitable full-disk spectrum was obtained with the Fourier transform spectrometer (FTS) at the Kitt Peak National Observatory Telescope (Fink and Larson 1979). Systematic studies were then pursued from Earth with four different instruments: the Kitt Peak FTS (Lemmon et al. 1993, 1995), the UKIRT and IRTF/CSHELL (Griffith et al. 1991; Griffith et al. 1998; Griffith et al. 2003), and the CFHT/FTS (Coustenis et al. 1995, 2001).

2.1.2 Speckle imagery

Speckle imaging (Labeyrie 1970; Matthews et al. 1996) is based on the acquisition of very short exposure images [typically 0.2 s for Titan in Gibbard et al. (1999)], to "freeze" the atmospheric turbulence and capture the light while it is still forming coherent interference patterns at the detector, which—by lack of long exposure—induces a low signal-to-noise ratio (SNR) and requires more centring–summing processes. Interferometry comes into play when the Fourier transforms from different exposures are combined together, increasing the SNR, and allowing the user to recover—by inverse Fourier transform of the result—an image of better resolution. Still, speckle interferometry processing, like AO deconvolution, can produce artefacts near sharp edges, such as Titan's limb. The first such cloud images are temptingly convincing (Gibbard et al. 2004a,b), even though bright features are visible in Gibbard et al. (1999) images without the authors mentionning them.

2.1.3 Adaptive optics (AO): imagery and spectro-imagery

The principle of adaptive optics (Babcock 1953) is based on the servo-control of a deformable mirror (correcting the turbulence) using a wavefront sensor (checking the state of the turbulence). The first Titan AO image was acquired at the observatory of la Silla, Chile (Saint-Pé et al. 1993), and many more AO systems have followed on this topic: in particular the 3.6-m ESO telescope (Combes et al. 1997), the CFHT (Coustenis et al. 2001, 2005; Hirtzig et al. 2005), the VLT (Gendron et al. 2004;

[1] Given Kuiper's technique (photographic spectroscopy), we know in retrospect that with repeated observations, he might have been able to detect large storms [at least as large as the ones described by Griffith et al. (1998) and Schaller et al. (2006a)], giving us the very first data on clouds six decades ago.

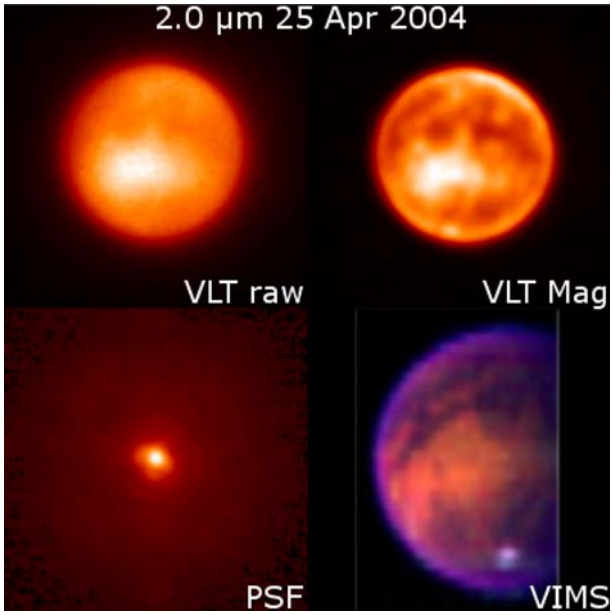

Fig. 1 Example of deconvolution. On the *upper left corner* is displayed a "raw" VLT/NACO image acquired on 25 April 2004 at 2.0 µm. On the *lower left corner* is the point-spread function (PSF) representing the remnants of the diffraction phenomena not corrected by the adaptive optics (AO) system. On the *upper right corner* is the result of the Magain deconvolution. The VIMS T0 false colour image (PIA 06404) in the *lower right corner* proves that all the features, barely visible on the "raw" image, but detected on the deconvolved one, are real

Hirtzig et al. 2006; Hirtzig et al. 2007; Ádámkovics et al. 2007), the Keck (Roe et al. 2002b; Bouchez and Brown 2005; de Pater et al. 2006; Ádámkovics et al. 2007), Palomar (Bouchez 2003), and Gemini (Roe et al. 2002a; Bouchez 2003; Schaller et al. 2006b).

Two techniques can be combined with AO: imagery and spectro-imagery. The former uses narrow-band filters to probe down to specific atmospheric levels of Titan, or all the way to the lowest atmosphere and surface, with a resolution of a few tens of kilometres in altitude. The latter, spectro-imagery, can take two slightly different forms: spatially-resolved spectroscopy (also mapping spectrometry) and integral field spectrometry (IFS). See Bouchez (2003) and Negrão et al. (2007) for more details on mapping spectroscopy; for examples of IFS see Hirtzig et al. (2005) (WHT/OASIS) or Ádámkovics et al. (2007) (VLT/SINFONI).

To enhance the contrast of AO images, deconvolution processes can be used to retrieve information close to the diffraction limit (Fig. 1), even though deconvolution is not mandatory for atmospheric features detection. This mathematical method produces a plausible image of Titan's disk before its blurring by the turbulence. In Combes et al. (1997), Coustenis et al. (2001), and Hirtzig et al. (2006), deconvolution methods like Lucy–Richardson (Bratsolis and Sigelle 2001), MISTRAL (Conan et al. 1998) or MCS (Magain et al. 1998) were applied to the data with great care so as not to over-interpret the results. Similarly, de Pater et al. (2005) use the AIDA

deconvolution method for some Keck images, and Meier et al. (2000) refer to the Wiener deconvolution (Kondo et al. 1977) for HST data. See Coustenis et al. (2001) and Hirtzig et al. (2006) for an example of enhancement of very faint features: the stratospheric haze enhancement occurring on Titan's morning limb.

Two drawbacks of the deconvolution methods must be mentioned here: the photometry is lost, and specific artefacts (such as Gibb's ring) must not be over-interpreted. Gibb's ring is an artificially brighter limb on Titan's disk (enhancing existing limb-brightening or dampening real dark-brightening), due to the Fourier transform signature of the frontier between Titan's edge and the sky in the background. Deconvolution methods will often enhance the contrast of this edge, producing a narrower-than-resolution but visible brighter ring over Titan's edge (and also negligible similar ripples inside and outside the disk). See http://www.lesia.obspm.fr/planeto/Titan/Titan_sol_ao/Index.html for more information.

2.2 From space: the HST and the spacecrafts

The first resolved image of Titan in the near-infrared was acquired by the Hubble Space Telescope in 1990 at 0.89 μm (Caldwell et al. 1992), with the wide-field planetary camera during early release observation. But these early data were obtained before the mirror correction of 1993 (STS-61), and were of poor quality. Further HST studies gathered many more Titan infrared images (Lorenz et al. 1997, 1999b; Lorenz 2002), with the first surface results in 1994 (Smith et al. 1996). At that time Titan's disk was divided into seven pixels, close to the theoretical resolution of the HST mirror (ten pixels on Titan's diameter at most); such a spatial resolution was too coarse to resolve clouds, but fine enough for monitoring the north–south asymmetry evolution by spectroscopy (Lorenz et al. 2004).

Spacecrafts like Voyager and Cassini–Huygens can be considered as another family of space observatories. Given their close distance to the target, they benefit from higher spatial resolution. The Pioneer and Voyager images were taken primarily in the visible (Lockwood et al. 1979; Smith et al. 1981, 1982). For infrared space imagery and spectro-imagery, we will mention herein three particular instruments aboard Cassini–Huygens: the ultraviolet-visible-infrared imager Cassini/ISS (Imaging Science Subsystem) (Porco et al. 2005), the Visible and Infrared Mapping Spectrometer Cassini/VIMS (Brown et al. 2006), and the Descent Imager/Spectral Radiometer Huygens/DISR (Tomasko et al. 2005).

3 Titan's atmospheric phenomena

Titan revolves around Saturn, whose orbit is inclined at 26°44″ to the ecliptic [see Stiles et al. (2008), Lorenz et al. (2008a) for further refinements]. Titan's atmosphere is therefore seasonally evolving during its $\simeq$30 years of revolution around the Sun. Using the observational techniques described in the previous section, features with characteristic lifetimes ranging from a day to a year have been detected on Titan: short-lived clouds and year-long cloud systems, diurnal and seasonal phenomena like the north–south asymmetry (e.g. Bouchez 2003; Hirtzig et al. 2006; Schaller et al.

2006a; Ádámkovics et al. 2007). We will focus hereafter on some of the atmospheric features detected, listed in Table 1. Their appellations may vary from one investigation to an other and, as we will show hereafter, their altitudes and other characteristics are extremely model-dependent. Thus, we will try herein to keep as much as possible of the model-independent wavelength information to make comparisons. Nevertheless the spectral response of the same cloud will vary, depending on the haze opacity and the lighting conditions (emission angle, incidence angle, and phase angle) of the observations. A radiative transfer analysis is needed to determine the cloud altitude, and make parameter comparisons between different latitudes, haze conditions, and lighting conditions. However, this comparison is viable for similar observing conditions.

3.1 North–south asymmetry

It has been well known since Voyager that Titan's atmosphere exhibits a different hemispheric asymmetry depending on the season (Fig. 2a). The hemisphere rich in aerosols appears brighter in the infrared, and darker in the visible, than its deprived counterpart. The winter hemisphere is aerosols-enriched in the lower atmosphere, because the polar night facilitates the condensation of larger and more numerous aerosol particles (Yung 1987; Rannou et al. 2002). Furthermore, in that polar region downward transport of aerosol particles to the troposphere is forced by the descending branch of the large-scale circulation (Rannou et al. 2004). In the visible, aerosols are dark, while they are bright in the infrared (Coll et al. 2003). At the time of the Voyager encounter (southern summer), Titan's southern hemisphere was bright in the visible, but dark in the infrared. Two Titan seasons later (13 years each), Cassini/Huygens witnessed a similar situation, with a northern limb that was dark in the visible, and bright in the infrared. The asymmetry was inverted at the time of the first AO and HST images, during the Titan's southern winter, with the famous "Titan's smile" (a bright southern limb) visible on all the infrared data (Coustenis et al. 2001; Lorenz et al. 2001).

From HST data in the visible, Lorenz et al. (1999b, 2001) showed that the asymmetry inversion was already occurring in the late 1990s. Additional data, from both the HST (Lorenz 2002; Young et al. 2002; Anderson et al. 2008) and the ground (Chanover et al. 2003; Anderson et al. 2004) proved that the reversal was occuring faster at higher altitudes. From AO images in the infrared, Ádámkovics et al. (2005) and Hirtzig et al. (2006) showed that the reversal was completed in 2002. Both teams concluded that this asymmetry reversal happened 2 years faster than the 7 years (90° in phase) value predicted by the models (Sromovsky et al. 1981) for the lag due to the thermal intertia of the atmosphere (Flasar and Conrath 1990).

Several mechanisms were proposed to explain the NSA (see Roos-Serote 2004 for a review), but dynamics seem to be the most plausible answer: Hutzell et al. (1993) showed that microphysics alone (via changes in chemical composition or in products concentration) cannot fully explain the NSA reversal. The spatial repartition of the haze, coupled with dynamical effects, can reproduce the changes in appearance of Titan's atmosphere as seasons go by (Hutzell et al. 1996; Lorenz et al. 1999b; Tokano et al. 1999; Richardson et al. 2007). Recent GCM models can even reproduce the 5-year settling period (see in particular Sect. 5 of Luz et al. 2003).

Table 1 Detections of transient clouds and other atmospheric features (from 1987 to 2006)

Date	Flyby	SPF	Clouds in general	Polar collar	Cloud cover (%)	Instrument	Reference
1987/05/27		None	None		0.0	CGAS/NASA's ITF	Griffith et al. (1998)
1990/07/25		None	None		0.0	CGAS/NASA's ITF	Griffith et al. (1998)
1993/09/13		None	None		0.0	CGS4/UKIRT	Griffith et al. (2000)
1993/09/30					0.2	CGS4/UKIRT	Griffith et al. (2000)
1993/09/30		None	None		0.0	CGS4/UKIRT	Griffith et al. (1998)
1993/10/07		None	None		0.0	CGS4/UKIRT	Griffith et al. (1998)
1995/09/04					7.0	CGS4/UKIRT	Griffith et al. (1998)
1995/09/05					9.0	CGS4/UKIRT	Griffith et al. (1998)
1996/09/06		SPF				Speckle NIRC/Keck	Gibbard et al. (2004a)
1997/07/27					0.6	CGS4/UKIRT	Griffith et al. (2000)
1997/08/27		None	None		0.0	CGS4/UKIRT	Griffith et al. (1998)
1997/08/28		None	None		0.0	CGS4/UKIRT	Griffith et al. (1998)
1997/10/10		SPF				Speckle NIRC/Keck	Gibbard et al. (2004a)
1997/10/11		SPF				Speckle NIRC/Keck	Gibbard et al. (2004a)
1997/10/13		SPF				Speckle NIRC/Keck	Gibbard et al. (2004a)
1997/10/17		None	None		0.0	CGS4/UKIRT	Griffith et al. (2000)
1997/10/26					0.3	CGS4/UKIRT	Griffith et al. (2000)
1997/10/26		None	None		0.0	CGS4/UKIRT	Griffith et al. (1998)
1998/07/27		SPF				Speckle NIRC/Keck	Gibbard et al. (2004a)
1998/07/29		SPF				Speckle NIRC/Keck	Gibbard et al. (2004a)
1998/07/30		SPF				Speckle NIRC/Keck	Gibbard et al. (2004a)
1998/07/31		SPF				Speckle NIRC/Keck	Gibbard et al. (2004a)
1998/08/01		SPF				Speckle NIRC/Keck	Gibbard et al. (2004a)

Table 1 continued

Date	Flyby	SPF	Clouds in general	Polar collar	Cloud cover (%)	Instrument	Reference
1998/10/07		SPF				Speckle NIRC/Keck	Gibbard et al. (2004a)
1998/10/08		SPF				Speckle NIRC/Keck	Gibbard et al. (2004a)
1998/10/09		SPF				Speckle NIRC/Keck	Gibbard et al. (2004a)
1998/10/10		SPF				Speckle NIRC/Keck	Gibbard et al. (2004a)
1998/10/14		SPF				Speckle NIRC/Keck	Gibbard et al. (2004a)
1999/09/14					0.0–0.5	CGS4/UKIRT	Griffith et al. (2000)
1999/09/18					0.4	CGS4/UKIRT	Griffith et al. (2000)
1999/09/22					0.3–0.7	CGS4/UKIRT	Griffith et al. (2000)
1999/09/23					0.2–0.3	CGS4/UKIRT	Griffith et al. (2000)
1999/09/27					0.2	CGS4/UKIRT	Griffith et al. (2000)
1999/09/30					0.2–0.4	CGS4/UKIRT	Griffith et al. (2000)
1999/10/30				Polar collar		KCAM/Keck	Roe et al. (2002b)
2000/08/17				Polar collar		SCAM/Keck	Roe et al. (2002b)
2001/02/21				Polar collar		SCAM/Keck	Roe et al. (2002b)
2001/12/03		SPF	?			NIRSPEC/Keck	Brown et al. (2002)
2001/12/05		SPF		Polar hood		PUEO/CFHT	Hirtzig et al. (2006)
2001/12/07		SPF	Clouds			Gemini	Roe et al. (2002a)
2001/12/09		SPF	None			Gemini	Roe et al. (2002a)
2001/12/10		77°S	?	Tropopause cirrus		NIRSPEC/Keck	Brown et al. (2002)
2001/12/11		77°S				NIRSPEC/Keck	Brown et al. (2002)
2001/12/18		SPF	Clouds			NIRC2/Keck	Roe et al. (2002a)
2001/12/20		SPF	Clouds			NIRC2/Keck	Roe et al. (2002a)
2001/12/20		77°S, 78°S	63°S			PHARO/Palomar	Bouchez and Brown (2005)

Table 1 continued

Date	Flyby	SPF	Clouds in general	Polar collar	Cloud cover (%)	Instrument	Reference
2001/12/21		SPF	80°S, 60°S			NIRC2/Keck	Roe et al. (2002a)
2002/02/28		SPF, 87°S	65°S			NIRC2/Keck	Brown et al. (2002)
2002/03/04		SPF	?			NIRC2/Keck	Brown et al. (2002)
2002/09/23		72°S				PHARO/Palomar	Bouchez and Brown (2005)
2002/09/24		73°S				PHARO/Palomar	Bouchez and Brown (2005)
2002/09/25		72°S, 81°S				PHARO/Palomar	Bouchez and Brown (2005)
2002/09/26		75°S, 80°S				PHARO/Palomar	Bouchez and Brown (2005)
2002/09/27		SPF				PHARO/Palomar	Bouchez and Brown (2005)
2002/11/13		SPF		Polar hood		PUEO/CFHT	Hirtzig et al. (2006)
2002/11/14		SPF				PHARO/Palomar	Bouchez and Brown (2005)
2002/11/14		SPF		Polar hood		PUEO/CFHT	Hirtzig et al. (2006)
2002/11/15		Poor data				PHARO/Palomar	Bouchez and Brown (2005)
2002/11/16		83°S				PHARO/Palomar	Bouchez and Brown (2005)
2002/11/17		79°S				PHARO/Palomar	Bouchez and Brown (2005)
2002/11/18		81°S				PHARO/Palomar	Bouchez and Brown (2005)
2002/11/20		SPF				NACO/VLT	Gendron et al. (2004)
2002/11/20		SPF		Polar hood		PUEO/CFHT	Hirtzig et al. (2006)
2002/11/20		SPF		Polar hood		NACO/VLT	Hirtzig et al. (2006)
2002/11/21		SPF		Polar hood		PUEO/CFHT	Hirtzig et al. (2006)
2002/11/25		SPF				NACO/VLT	Gendron et al. (2004)
2002/11/25		SPF		Polar hood		NACO/VLT	Hirtzig et al. (2006)
2002/11/26		SPF				NACO/VLT	Gendron et al. (2004)
2002/11/26		SPF		Polar hood		NACO/VLT	Hirtzig et al. (2006)

Table 1 continued

Date	Flyby	SPF	Clouds in general	Polar collar	Cloud cover (%)	Instrument	Reference
2002/12/24		82°S				PHARO/Palomar	Bouchez and Brown (2005)
2002/12/27		72°S				PHARO/Palomar	Bouchez and Brown (2005)
2002/12/28		77°S				PHARO/Palomar	Bouchez and Brown (2005)
2003/01/12		82°S				PHARO/Palomar	Bouchez and Brown (2005)
2003/01/14		71°S, 83°S	58°S			PHARO/Palomar	Bouchez and Brown (2005)
2003/03/07		None				NIRC2/Keck	Gibbard et al. (2003)
2003/03/08		None				NIRC2/Keck	Gibbard et al. (2003)
2003/09/17		SPF				NIRC2/Keck	Schaller et al. (2006b)
2003/10/10		SPF				NIRC2/Keck	Schaller et al. (2006b)
2003/10/11		SPF				NIRC2/Keck	Schaller et al. (2006b)
2003/10/12		SPF				NIRC2/Keck	Schaller et al. (2006b)
2003/11/09		SPF				NIRC2/Keck	Schaller et al. (2006b)
2003/11/11		SPF				NIRC2/Keck	Schaller et al. (2006b)
2003/11/12		SPF				NIRC2/Keck	Schaller et al. (2006b)
2003/11/13		SPF				NIRC2/Keck	Schaller et al. (2006b)
2003/11/14		SPF				NIRC2/Keck	Schaller et al. (2006b)
2003/11/15		SPF				Gemini	Schaller et al. (2006b)
2003/11/17		SPF				Gemini	Schaller et al. (2006b)
2003/11/18		SPF				NIRC2/Keck	Schaller et al. (2006b)
2003/12/10		SPF				NIRC2/Keck	Schaller et al. (2006b)
2003/12/15		SPF				NIRC2/Keck	Schaller et al. (2006b)
2003/12/17		SPF				NIRC2/Keck	Schaller et al. (2006b)
2003/12/18		SPF				NIRC2/Keck	Schaller et al. (2006b)
2003/12/18		SPF	x1			NIRC2/Keck	Roe et al. (2005a)

Table 1 continued

Date	Flyby	SPF	Clouds in general	Polar collar	Cloud cover (%)	Instrument	Reference
2003/12/24		SPF				NIRC2/Keck	Schaller et al. (2006b)
2003/12/25		none				NIRC2/Keck	Schaller et al. (2006b)
2003/12/26		SPF				NIRC2/Keck	Schaller et al. (2006b)
2003/12/27		SPF				NIRC2/Keck	Schaller et al. (2006b)
2004/01/07		SPF				PUEO/CFHT	Hirtzig et al. (2006)
2004/01/08		SPF				PUEO/CFHT	Hirtzig et al. (2006)
2004/01/10		SPF				NIRC2/Keck	Schaller et al. (2006b)
2004/04/04		SPF				Gemini	Schaller et al. (2006b)
2004/04/04		SPF				Gemini	Roe et al. (2005a)
2004/04/05		SPF				Gemini	Schaller et al. (2006b)
2004/04/05		SPF				Gemini	Roe et al. (2005a)
2004/04/06		SPF				Gemini	Schaller et al. (2006b)
2004/04/06		SPF				Gemini	Roe et al. (2005a)
2004/04/07		SPF				Gemini	Schaller et al. (2006b)
2004/04/07		SPF				Gemini	Roe et al. (2005a)
2004/04/08		SPF				Gemini	Schaller et al. (2006b)
2004/04/08		SPF	x1			Gemini	Roe et al. (2005a)
2004/04/09		SPF				Gemini	Schaller et al. (2006b)
2004/04/09		SPF	x1			Gemini	Roe et al. (2005a)
2004/04/25		SPF				NACO/VLT	Hirtzig et al. (2006)
2004/04/26		SPF				NACO/VLT	Hirtzig et al. (2006)
2004/04/30		SPF				Gemini	Schaller et al. (2006b)
2004/04/30		SPF				Gemini	Roe et al. (2005a)

Table 1 continued

Date	Flyby	SPF	Clouds in general	Polar collar	Cloud cover (%)	Instrument	Reference
2004/05/04		none				Gemini	Schaller et al. (2006b)
2004/05/04		SPF	x1			Gemini	Roe et al. (2005a)
2004/05/05		SPF				Gemini	Schaller et al. (2006b)
2004/05/05		SPF	x1			Gemini	Roe et al. (2005a)
2004/05/06		SPF				Gemini	Schaller et al. (2006b)
2004/05/06		SPF				Gemini	Roe et al. (2005a)
2004/05/07		SPF				Gemini	Schaller et al. (2006b)
2004/05/07		SPF				Gemini	Roe et al. (2005a)
2004/07/02		SPF				ISS/Cassini	Porco et al. (2005)
2004/09/02		SPF				NIRC2/Keck	Schaller et al. (2006b)
2004/09/02		SPF	x2			NIRC2/Keck	Roe et al. (2005a)
2004/09/28		SPF				NIRC2/Keck	Schaller et al. (2006a)
2004/09/28		SPF				NIRC2/Keck	Schaller et al. (2006b)
2004/10/02		SPF				NIRC2/Keck	Schaller et al. (2006a)
2004/10/02		SPF				NIRC2/Keck	Schaller et al. (2006b)
2004/10/03		SPF				NIRC2/Keck	Schaller et al. (2006a)
2004/10/03		SPF				NIRC2/Keck	Schaller et al. (2006b)
2004/10/07		SPF				NIRC2/Keck	Schaller et al. (2006a)
2004/10/07		SPF				NIRC2/Keck	Schaller et al. (2006b)
2004/10/08		SPF				NIRC2/Keck	Schaller et al. (2006a)
2004/10/08		SPF				NIRC2/Keck	Schaller et al. (2006b)
2004/10/23		SPF				NIRC2/Keck	Schaller et al. (2006a)
2004/10/23		SPF				NIRC2/Keck	Schaller et al. (2006b)

Table 1 continued

Date	Flyby	SPF	Clouds in general	Polar collar	Cloud cover (%)	Instrument	Reference
2004/10/23		SPF	43°S			ISS/Cassini	Porco et al. (2005)
2004/10/24		SPF				Gemini	Schaller et al. (2006b)
2004/10/25		SPF	65°S			ISS/Cassini	Porco et al. (2005)
2004/10/26	TA=S5	SPF	40°S			VIMS/Cassini	Rodriguez et al. (2009)
2004/10/28		SPF				NIRC2/Keck	Schaller et al. (2006b)
2004/11/01		SPF				Gemini	Schaller et al. (2006b)
2004/11/02		SPF				Gemini	Schaller et al. (2006b)
2004/11/03		SPF				NIRC2/Keck	Schaller et al. (2006b)
2004/11/04		SPF				Gemini	Schaller et al. (2006b)
2004/11/05		SPF				Gemini	Schaller et al. (2006b)
2004/11/27		SPF				NIRC2/Keck	Schaller et al. (2006b)
2004/12/10			40°S			ISS/Cassini	Porco et al. (2005)
2004/12/13	TB=S6		41°S, 43°S, 47°S, 61°S			VIMS/Cassini	Griffith et al. (2005)
2004/12/13	TB=S6	SPF	40°S, N limb			VIMS/Cassini	Rodriguez et al. (2009)
2004/12/13	TB=S6	SPF	40°S			VIMS/Cassini	Barnes et al. (private communication)
2004/12/13	TB=S6		Ethane 70°N			VIMS/Cassini	Griffith et al. (2006)
2004/12/21		None				Gemini	Schaller et al. (2006b)
2004/12/24		None				Gemini	Schaller et al. (2006b)
2004/12/25		None				Gemini	Schaller et al. (2006b)
2004/12/27		None				Gemini	Schaller et al. (2006b)
2005/01/14		None				NIRC2/Keck	Schaller et al. (2006b)
2005/01/14	TC=S7					VIMS/Cassini	Rodriguez et al. (2009)
2005/01/14		None				NIRC2/Keck	de Pater et al. (2006)

Table 1 continued

Date	Flyby	SPF	Clouds in general	Polar collar	Cloud cover (%)	Instrument	Reference
2005/01/15		None				NACO/VLT	Hirtzig et al. (2006)
2005/01/15		SPF				NIRC2/Keck	de Pater et al. (2006)
2005/01/16		None				Gemini	Schaller et al. (2006b)
2005/01/16		?				NACO/VLT	Hirtzig et al. (2006)
2005/01/16		?				NACO/VLT	Hirtzig et al. (2007)
2005/01/16		SPF				NIRC2/Keck	de Pater et al. (2006)
2005/01/17		SPF				NIRC2/Keck	de Pater et al. (2006)
2005/01/20		SPF				NIRC2/Keck	Schaller et al. (2006b)
2005/01/20		SPF				NIRC2/Keck	de Pater et al. (2006)
2005/01/23		None				Gemini	Schaller et al. (2006b)
2005/01/24		None				Gemini	Schaller et al. (2006b)
2005/01/25		None				Gemini	Schaller et al. (2006b)
2005/01/28		None				Gemini	Schaller et al. (2006b)
2005/02/08		None				Gemini	Schaller et al. (2006b)
2005/02/09		None				Gemini	Schaller et al. (2006b)
2005/02/10		None				Gemini	Schaller et al. (2006b)
2005/02/12		None				Gemini	Schaller et al. (2006b)
2005/02/14		None				NIRC2/Keck	Schaller et al. (2006b)
2005/02/15		None				NIRC2/Keck	Schaller et al. (2006b)
2005/02/15	T3=S8		N limb			VIMS/Cassini	Rodriguez et al. (2009)
2005/02/16		None				Gemini	Schaller et al. (2006b)
2005/02/19		None				Gemini	Schaller et al. (2006b)
2005/02/20		None				Gemini	Schaller et al. (2006b)

Table 1 continued

Date	Flyby	SPF	Clouds in general	Polar collar	Cloud cover (%)	Instrument	Reference
2005/02/21		None				Gemini	Schaller et al. (2006b)
2005/02/22		None				Gemini	Schaller et al. (2006b)
2005/02/25		None				Gemini	Schaller et al. (2006b)
2005/03/01		None				Gemini	Schaller et al. (2006b)
2005/03/02		None				Gemini	Schaller et al. (2006b)
2005/03/04		None				Gemini	Schaller et al. (2006b)
2005/03/05		None				Gemini	Schaller et al. (2006b)
2005/03/09		None				Gemini	Schaller et al. (2006b)
2005/03/24		None				Gemini	Schaller et al. (2006b)
2005/03/31	T4=S9					VIMS/Cassini	Rodriguez et al. (2009)
2005/04/16	T5=S10					VIMS/Cassini	Rodriguez et al. (2009)
2005/08/21	T6=S13		Ethane 70°N			VIMS/Cassini	Griffith et al. (2006)
2005/08/22	T6=S13					VIMS/Cassini	Rodriguez et al. (2009)
2005/08/22	T6=S13		Ethane 70°N			VIMS/Cassini	Griffith et al. (2006)
2005/09/07	T7=S14					VIMS/Cassini	Rodriguez et al. (2009)
2005/09/07	T7=S14		Ethane 70°N			VIMS/Cassini	Griffith et al. (2006)
2005/09/29		SPF				NIRC2/Keck	Schaller et al. (2006b)
2005/10/09		SPF				OSIRIS/Keck	Schaller et al. (2006b)
2005/10/10		SPF				OSIRIS/Keck	Schaller et al. (2006b)
2005/10/27	T8=S15		?			VIMS/Cassini	Rodriguez et al. (2009)
2005/11/21		None				OSIRIS/Keck	Schaller et al. (2006b)
2005/11/22		None				OSIRIS/Keck	Schaller et al. (2006b)
2005/11/24		None				OSIRIS/Keck	Schaller et al. (2006b)

Table 1 continued

Date	Flyby	SPF	Clouds in general	Polar collar	Cloud cover (%)	Instrument	Reference
2005/12/24		SPF				NIRC2/Keck	Schaller et al. (2006b)
2005/12/26	T9=S17	SPF				VIMS/Cassini	Rodriguez et al. (2009)
2006/01/15	T10=S17		40°N, N limb			VIMS/Cassini	Rodriguez et al. (2009)
2006/02/27	T11=S18					VIMS/Cassini	Rodriguez et al. (2009)
2006/03/18	T12=S19					VIMS/Cassini	Rodriguez et al. (2009)
2006/04/30	T13=S20					VIMS/Cassini	Rodriguez et al. (2009)
2006/05/20	T14=S20					VIMS/Cassini	Rodriguez et al. (2009)
2006/07/02	T15=S21		?			VIMS/Cassini	Rodriguez et al. (2009)
2006/07/22	T16=S22		40°S			VIMS/Cassini	Rodriguez et al. (2009)
2006/09/07	T17=S23		40°S			VIMS/Cassini	Rodriguez et al. (2009)
2006/09/23	T18=S23		?			VIMS/Cassini	Rodriguez et al. (2009)
2006/10/09	T19=S24					VIMS/Cassini	Rodriguez et al. (2009)
2006/10/25	T20=S25		40°S			VIMS/Cassini	Rodriguez et al. (2009)

The first column indicates the date of the observation as well as, when relevant, the flyby number for the Cassini orbiter. The middle panel enumerates rapidly the reports of atmospheric features: South Polar Feature (at the south pole within the error bars "SPF", undoubtedly absent "none"; other bright features poleward of 70°S will be reported here with their latitudes), clouds at other latitudes (with their latitude when available, number of bright features if no coordinate system was given, "?" if faint features are visible but not explicitely imputable to clouds), polar collars (their name is given according to the observers' denomination), and percentage of cloud cover when available (the only value available for full-disk spectroscopy, but sometimes estimated for spatially resolved clouds). The last panel returns the instrument used for the observations, as well as the reference where the data were discussed

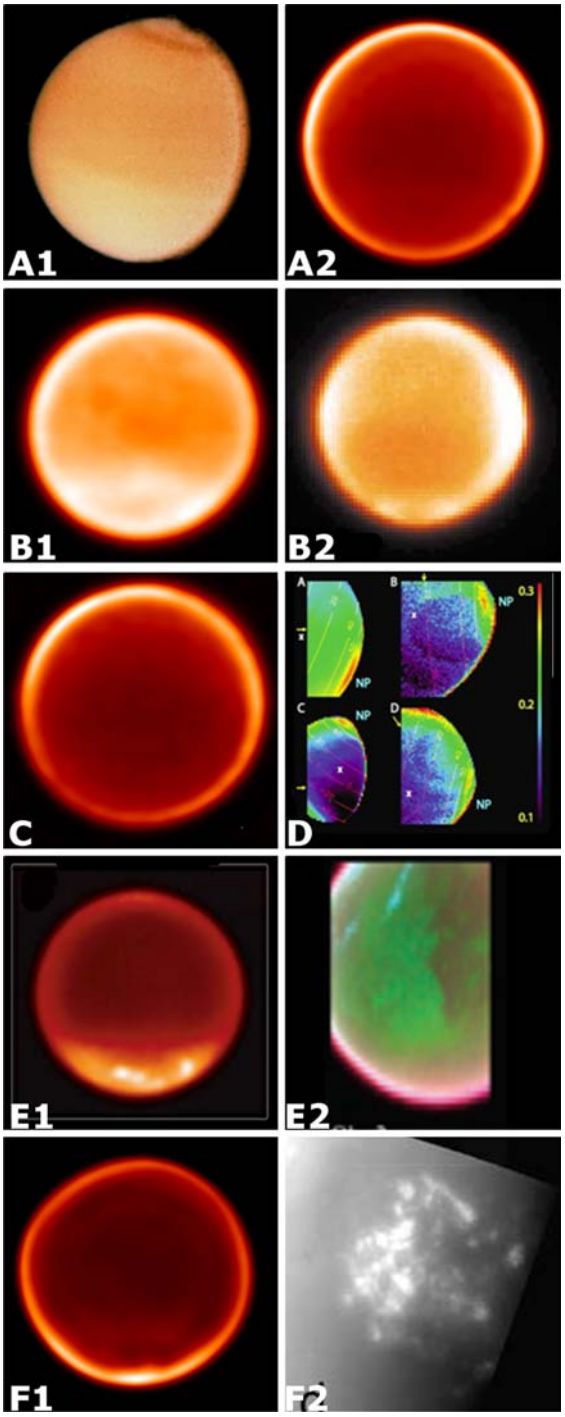
A1
A2
B1
B2
C
A
B
NP
0.3
C
NP
D
0.2
NP
0.1
D
E1
E2
F1
F2

◀ **Fig. 2** Sample images of atmospheric features. Panels **a1** and **a2** illustrate the north–south asymmetry: a bright southern hemisphere in the visible witnessed by Voyager 2 (**a1**, composite of *blue*, *green*, and *violet* channels, 23 August 1981, Smith et al. 1982) and the same season observed with AO in the infrared with a bright northern limb (**a2**, VLT, 1.64 μm, 26 November 2002, Gendron et al. 2004). Panels **b** display two similar views of the "tropopause cirrus" (**b1**, VLT, 1.04 μm, 26 November 2002, Gendron et al. 2004) and the "polar collar" (**b2**, Keck, 1.702 μm, 20 February 2001, Roe et al. 2002b) at the south pole of Titan. Excerpt **c** (VLT, 2.17 μm, 16 January 2005, Hirtzig et al. 2006) shows a bright morning limb (West, on the *left*) although a feeble phase effect was expected on the evening limb, evidence for a stratospheric condensation of haze (Coustenis et al. 2001). Sub-pictures from panel **d** are 2.8 μm images of the stratospheric "ethane cloud" detected by Cassini/VIMS at the northern limb of Titan (Griffith et al. 2006). Panels **e1** and **e2** show the aspects of the mid-latitude methane clouds unresolved from Earth (E1, Keck, 2.108 μm, 21 December 2001, Roe et al. 2002a) and resolved with Cassini/VIMS (E2, RGB colours composite of 2.3, 2.0, and 2.13 μm channels, 13 December 2004, Griffith et al. 2005). Similarly, panels **f1** and **f2** show the gathering of methane clouds at the south pole (named SPCS herein) from the Earth (**f1**, VLT, 2.12 μm, 26 November 2002) and with Cassini/ISS (**f2**, 928 nm, 2 July 2004, Porco et al. 2005). Furthermore, the SPCS "companions" (Hirtzig et al. 2006) can be detected on both sides of the southern limb on the **f1** image, with an appearance closely similar to the one of the "tropopause cirrus" on **b1** taken during the same observation run

3.2 Polar "collars" and caps

Since the early 1980s thanks to the Voyager flyby, "collars" and/or "hoods" have been reported close to the poles of Titan, like a dark ring on Voyager 1 images above 60°N (Smith et al. 1982), and as early as 1994 with the first ground-based resolved images of Saturn's satellite, like on Fig. 2b. We need to determine if these phenomena are different, linked, similar or identical to each other.

Brown (2000), Roe et al. (2000, 2002a), and Hirtzig et al. (2006); Hirtzig et al. (2007) observations show a "collar" close to the south (summer) pole, from limb to limb along the 70°S parallel. Brown et al. (2002) also refer to a "tropopause cirrus" that is needed to improve the fit to the NIRSPEC spectra of Titan in the 2.0–2.3 μm range. The infrared filters or wavelengths where these phenomena were detected are reported in Table 2.

Like its southern counterpart, the northern limb of Titan has exhibited several "collars" and/or "hoods". Voyager 2 images in the visible showed in 1980 a dark collar (Smith et al. 1982) close to 70°N (in spring at that time). Lorenz et al. (2006) reported its slow disappearance, witnessed by the UV camera aboard HST. Roe et al. (2002a) also underline a cap above the north pole in 1999–2001, bright in specific infrared Keck images: it is bright at 1.702 μm, but invisible at 1.158 μm.

3.3 Diurnal changes: stratospheric haze enhancement in Titan's morning limb

One of the phenomena occurring in Titan's atmosphere is particularly subtle and requires fine conditions to be observed. Coustenis et al. (2001) followed by Hirtzig et al. (2006) proved the existence of a nocturnal condensation of aerosols or haze in the stratosphere during the night of Titan. It can be observed only in cases of very low phase angles (+0.25°E at best), when the western (morning) limb is brighter than the eastern one (where the phase effect should be). This is readily seen on the deconvolved images [see Fig. 3 of Hirtzig et al. (2006)] but it is also visible on other data, like the

Table 2 Detections of the south polar cloud system and of polar "collars" from various observations in southern summer

Filter	Band	SPCS	Collar observation
Surface			
VLT/IB_2.00 (2.000±0.030 μm)	K	Faint[(c2)]	None c2
Troposphere			
VLT/NB_2.12 (2.120±0.010 μm)	K	Bright[(b,c2)]	Faint S Cap[(b,c2,d)]
CFHT/$H_{2(1--0)}$ (2.122± 0.010 μm)	K	Bright[(c2)]	S Cap[(c2)]
VLT/IB_2.15 (2.150±0.015 μm)	K	Faint[(c2)]	Faint S Cap[(d)]
Tropopause			
VLT/NB_1.04 (1.040±0.007 μm)	I		Bright S Cap[(b)]
CFHT/Paschenγ (1.094±0.005 μm)	I		Bright S cap[(c2)]
VLT/NB_1.24 (1.237±0.008 μm)	J		S Collar[(b)]
Stratosphere			
Keck/H1702 (1.702±0.008 μm)	H		Bright S Collar+N limb-brightening[(a)]
VLT/NB_1.64 (1.644±0.009 μm)	H		Faint S cap + Faint N cap[(b)]
Keck/J1158 (1.158±0.009 μm)	J		Bright S Collar[(a)]
CFHT/J2 (1.181±0.064 μm)	J		Faint S collar[(c1)]
VLT/NB_2.17 (2.166±0.010 μm)	K	None[(b,c2)]	None[(b,c1,d)]

Filters are sorted by increasing altitude. Numerical values are not given regarding the altitudes probed by each filter, since this is extremely model-dependent; nevertheless all the models agree on this sorting by altitude. Broad-band filters are not included here, since they are not altitude-specific, as well as images where the SPCS would be merged into a bright southern limb. References used here are: [(a)] Fig. 1 in Roe et al. (2002a), [(b)] Fig. 2 in Gendron et al. (2004), [(c1)] Fig. 3 and [(c2)] Fig. 5 in Hirtzig et al. (2006), [(d)] Fig. 1 in Hirtzig et al. (2007)

Keck images of Brown (2005) and de Pater et al. (2005) or on some HST images (Young, private communication).

Microphysical models of Titans haze (e.g. Rannou et al. (2006) and references within) predict the condensation of methane by-products (such as ethane and acetylene as the most abundant ones) somewhere between 70 and 90 km of altitude in the polar regions (Coustenis et al. 2001). Since on Titan one night lasts about 8 terrestrial days, even considering stratospheric winds of about 100 m/s (Hubbard et al. 1993; Kostiuk et al. 2001, 2005, 2006; Luz et al. 2005; Moreno et al. 2005; Sicardy et al. 2006, 1999) that would shorten the length of the night to 1 Earth day for the particles at that altitude, there is enough time for the condensation to occur at the lower temperatures prevailing on the night side (Lindal et al. 1983; Flasar 1983; Lellouch et al. 1989). If condensation nuclei are present, only a few 10^{-5} s are needed to begin the condensation (Pruppacher and Klett 1978). This nocturnal condensation then manifests itself by a brighter colder morning limb with respect to the darker warmer evening side.

The general circulation model developed for the atmosphere of Titan at the Institute Pierre-Simon Laplace (Hourdin et al. 1995, 2004; Lebonnois et al. 2001, 2003;

Rannou et al. 2002, 2004, 2006; Crespin et al. 2008) can give a cloud production from temperature variations reaching 0.1°–0.2°K in regions of supersaturation, and GCM modellers are investigating the temperature variation we can expect on Titan between the day and night hemispheres.

3.4 Methane drizzle in the troposphere

Using the Integral Field Spectrometer (IFS) SINFONI/VLT, Ádámkovics et al. (2007) noticed that, after comparison of the surface contribution (in the core of the 2 μm window) with a combination of surface and low tropospheric ones at slightly longer wavelengths, there appeared a lack of infrared emission in the low troposphere probably due to an enhancement of scattering particles near the morning limb. These results are consistent with the indirect finding by Huygens of a thin liquid methane–nitrogen cloud close to the surface, at about 21 km of altitude (Tomasko et al. 2005; Tokano et al. 2006b; Tokano et al. 2006a).

The modelling of the SINFONI/VLT data required a VIMS map extrapolation for the surface contribution, a polar hood of haze, variation of the aerosol profile as a function of latitude, and DISR results describing the vertical profile of the atmosphere. It is unclear whether the authors took also into account phase effects, alhtough east–west asymmetries are known to be highly dependent on the phase angle, that can possibly blur subtle features such as the "morning haze" (Hirtzig et al. 2006). From this model, the upper altitude and density of the scatterers were determined: about 1.6 cm^3/cm^2 at $\simeq$30 km, leading to a particle size of the order of 1 μm, compatible with liquid methane droplets, probably present in the saturated troposphere witnessed by Huygens.

This mist or drizzle of liquid methane may then be either one source for the cloud material (via advection by large-scale winds), or one final state of the disaggregating "transient clouds". Ádámkovics et al. (2007) favour a mechanism similar to the "morning stratospheric haze enhancement" (Coustenis et al. 2001; Hirtzig et al. 2006), relying on the nocturnal condensation of atmospheric material during the night, with a probable influence of the topography to either maintain or evaporate or precipitate the drizzle during daylight.

It is worth noting that Kim et al. (2008) discard the entire study because of possible processing artefacts over-interpretation. Moreover, Griffith et al. (2008) conclude that Titan's tropical atmosphere is dry, another aspect contradictory with the drizzle hypothesis. Eventually, Cassini RADAR failed to detect directly such a drizzle (Lorenz et al. 2008b).

4 Titan's clouds

4.1 Spatially unresolved clouds

Cloud activity on Titan was first reported via full-disk spectroscopy from data taken on the 30 September 1993 with UKIRT. Griffith et al. (1998) witnessed dramatic changes in Titan's brightness at 1.6 and 2.0 μm, wavelengths probing down to the troposphere, with a maximum variation of up to 200%. With the same method, Griffith et al. (2000)

found other spectral signatures of clouds in 1995, 1997, and 1999, but with lesser impact on the albedo.

Since these data concerned Titan's disk as a whole, no information could be retrieved on the coordinates of the cloud, or even on its uniqueness. The Griffith et al. (1998) analysis of the data placed it near the equator, based on spectral changes from one night to the next, even though one cannot exclude that the feature was deforming, similarly to the clouds around the south pole resolved by Cassini/ISS for instance (see Sect. 4.2.1). Griffith et al. (1998) inferred a 7–9% coverage of clouds located at $\simeq$16 km. In such a case, we could be dealing with an event similar to the one underlined by Schaller et al. (2006a): a large outburst of cloud activity. The altitude of the fainter clouds detected by Griffith et al. (2000) seems to be slightly higher, at $\simeq$27 km.

Since that first detection, disk-resolved observations of Titan have permitted several direct viewings of clouds at various locations in Titan's atmosphere, observed directly either by Adaptive Optics, by the HST, or by the Cassini–Huygens mission.

4.2 Titan clouds at the south pole

4.2.1 The south polar cloud system (SPCS)

The south polar cloud system (SPCS) has been detected from the ground as a large polar feature hovering above Titan's south pole, seen regularly between 1996 and 2006 (Gibbard et al. 1999, 2003; Brown et al. 2002; Roe et al. 2002a; Roe et al. 2002b; Bouchez 2003; Gendron et al. 2004; Schaller et al. 2004; Schaller et al. 2006b; Bouchez and Brown 2005; Hirtzig 2005; Hirtzig et al. 2006; Hirtzig et al. 2007). From Earth, the SPCS was visible in particular at 2 μm (but never at wavelengths longer than 2.17 μm, which sets constraints on the feature's altitude, below $\simeq$50 km as explained in Hirtzig et al. (2006), Schaller et al. (2006b), and Hirtzig et al. (2007) and reported in Table 2). Brown et al. (2002) compare two 2.0–2.3 μm spectra of the SPCS on one hand and a surface feature close to the SPCS on the other hand, showing that the two spectra diverge shortward of 2.155 μm, in the low atmosphere.

Cassini/ISS has gathered images of the SPCS with exquisite detail in some occasions since July 2004 (Porco et al. 2005): the SPCS is a vast system of smaller cloud features, appearing and disappearing randomly in the same region (poleward of the 70thS parallel), resembling cumulus convection, that cannot be resolved from Earth. Cassini/VIMS also resolved the feature at longer wavelengths, confirming also the spectral signature of the SPCS reported from Earth: it is bright from 2.002 to 2.152 μm, and faint in the 2.168 μm channel (see Brown et al. 2006; Rodriguez et al. 2009 and Fig. 3).

The clouds detected in 1993 (Griffith et al. 2000) may or may not have been this SPCS. The first speckle image of the SPCS possibly dates back to September 1996 (Gibbard et al. 1999, 2004a), while nearly simultaneous AO images of the SPCS were acquired in December 2001 with the Keck/NIRSPEC (Brown et al. 2002) and the CFHT/PUEO (Hirtzig et al. 2006).

Given the spatial resolution of the larger ground-based telescopes, the SPCS appears to be $\simeq$1,000 km wide (5 pixels at the CFHT). Computations of cloud coverage vary

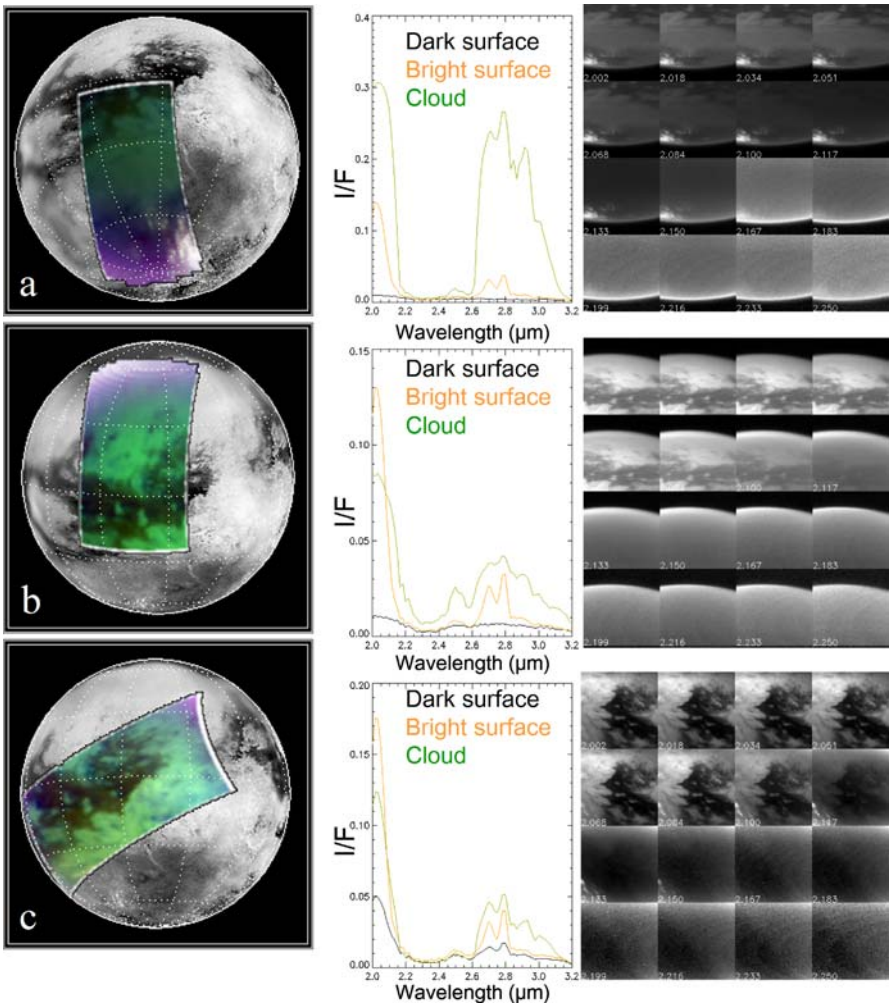

Fig. 3 Excerpts of spectro-imagery VIMS data for three types of clouds. These datacubes are taken from the S05 (**a**, **b**) and S06 (**c**) datasets (26 October and 13 December 2004). The upper panel **a** corresponds to the SPCS (76°E, 75°S), the intermediate panel illustrates the "ethane cloud"/NPCS (133°E, 58°N), while the lower panel relates the same study for a "zonal streak" (173°E, 41°S). In the left column is a projection of the current VIMS datacube (colour composite $R = 1.6/1.3$, $G = 2.0/1.3$, $B = 1.3/1.08\,\mu$m) over the spherical shape of Titan (mapped with a grey-scale 0.93 μm ISS map); meridians and parallel are shown every 30°. The middle panel displays the spectra of dark (in *black*), bright (in *orange*) and cloud (in *green*) pixels in the 2.0–3.2 μm range. Finally, the right panel shows the 16 images of the cube between 2.002 and 2.250 μm and their wavelengths. Those clouds did not have the same spectral response, even though observing conditions were similar ($\simeq$14° phase angle, 70°–90° observing angle). For instance, the SPCS **a** is obvious from 2.002 to 2.152 μm, and faint at 2.168 μm (and perhaps even decipherable at longer wavelengths here). The "ethane cloud"/NPCS **b** appears as a bright limb from 2.068 to 2.152 μm, while a regular limb-brightening would appear only longward of 2.168 μm. Regarding the "zonal streak" **c**, it is visible from 2.002 to 2.133 μm, faint at 2.152 μm, and invisible at 2.168 μm. On the spectra, other discrepancies appear: e.g. the lack of signature of the "zonal streak" in the 2.5 μm region, where only high-altitude atmospheric features can enhance the very narrow "window". In the 2.3 μm area, the "ethane cloud"/NPCS **b** spectrum differs from the eight others because the NPCS is very close to the limb

greatly in the literature, a sign of high variability in cloud activity. Based on the resolving power of the VLT, Hirtzig et al. (2006) found a 4–5% maximum cloud cover in November 2002. Assuming that the 0.1–1.1% flux contribution of the unresolved features could be attributable to 100–400-km-wide clouds (Brown et al. 2002), Bouchez and Brown (2005) concluded on a 0.2–0.6% coverage in the fall of 2002. This value is compatible with the ones deduced by spectroscopy in Griffith et al. (2000) but considerably smaller than the 7% coverage in Griffith et al. (1998).

Schaller et al. (2004) and Schaller et al. (2006b) showed that the cloud activity within the SPCS was evolving, with surges of brightness (November 2003 and November 2004) and periods of calm (early 2005). All the authors agree that there was a sudden decrease of activity in January 2005: in particular, ground-based observations during the Huygens probe descent (de Pater et al. 2006; Schaller et al. 2006b) revealed that the probe encountered a quiescent period in terms of cloud activity, and no visible cloud was observed anywhere on Titan, although the SPSC was frequently detected two months before the Huygens descent (Schaller et al. 2006b).

Cassini/VIMS and Cassini/ISS images showed a weak rebirth of clouds in October 2005 at the south pole, that lasted only 2 months. Faint patches appeared again in October 2006 and in January–April 2007, till a new outburst in June 2007: this event lasted less than 2 weeks. Till October 2008, the SPCS was not observed again. From all these data, there may be a 9-month periodicity in the SPCS activity (Rodriguez et al. 2009).

4.2.2 The case of the SPCS companions

In all AO Hirtzig et al. (2006) images, the SPCS feature is often paired with two unmoving companions on each side of the limb. They are neither moving nor changing in shape, yet one is always larger than the other, certainly enhanced by phase effects. The companions are visible at slightly longer wavelengths than the SPCS: they are visible at 2.12 μm (as the SPCS is), but also at 2.15 μm (while the SPCS fades out), and merge into the brightened-limb at 2.17 μm [as noted already in Gendron et al. (2004)]. From this simple observation, the companions are deduced to be probably located at higher altitudes than the SPCS. This spectral behaviour corresponds to the one of the "tropopause cirrus" (Sect. 3.2).

4.3 Titan clouds at mid-latitudes

We focus here on clouds appearing northward of 70°S. Such "transient clouds" are observed at various latitudes and longitudes, mostly in tropospheric filters, as reported by Brown et al. (2002), Roe et al. (2002b), Gibbard et al. (2003), Bouchez (2003), Bouchez and Brown (2005), and Porco et al. (2005). At 35°–40°N, the HST had also detected possible clouds (Lorenz et al. 1999a, 2000). Porco et al. (2005) propose another class of elongated clouds called "zonal streaks", visible in Cassini/ISS data, also on Cassini/VIMS images (Griffith et al. 2005; Baines et al. 2005). Most of the Cassini clouds seem to be elongated longitudinally as if drifting with/carried by

the wind. However, it is not established that all these clouds are elongated. From the Earth, the elongated shape of the majority of these clouds cannot be easily resolved, and we may have to wait for the extremely large telescope with a diameter of a few dozen metres to constrain the shape. Until then, clouds mainly appear as tiny spots on Titan's disk, and we can only look for differences in spectral behaviour to differentiate or reunite those two types of clouds, round or elongated. From the Earth, only Roe et al. (2005a) were able to resolve elongated clouds along the 40th S parallel.

Most detections occur at mid-latitudes, around 40°S as noted in Roe et al. (2005a). As far as the longitude distribution of the clouds is concerned, Roe et al. (2005b) suggested that their detections could be usually located eastward of 150°W and westward of 60°E. Cassini images (Rodriguez et al. 2009) indeed confirm the accumulation of data points at specific latitudes; nevertheless in these data clouds were found at other longitudes than reported in Roe et al. (2005b), with accumulation of data at other longitudes. The 30° shift in the cloud distribution between the former and the latter works, focused on different epochs (2003–2004 and 2005–2007, respectively) strongly suggest some dynamical control by the atmosphere, and not orographic links.

From spectroscopic data, particularly by Cassini/VIMS, it is found that the spectral signatures of the clouds sometimes differ from each other (Griffith et al. 2005; Rodriguez et al. 2009). Figure 3 shows one such variation: as reported in Sect. 4.2.1, the SPCS (upper panel) is visible at 2.002–2.152 μm and faintly at 2.168 μm; the "zonal streak" is visible from 2.002 to 2.133 μm, faintly at 2.152 μm, and is scarcely detectable at 2.168 μm (with a poor signal-to-noise ratio of 1). This will constrain the altitude, the nature of the cloud, or both.

It is surprising that such occasional features were never seen by Combes et al. (1997) or Coustenis et al. (2001), Hirtzig et al. (2006); Hirtzig et al. (2007), compared for instance to Keck images (Roe et al. 2002a). The CFHT cannot resolve clouds smaller than 300 km (600 km with respect to Shannon's principle[2]), but the VLT benefits from an angular resolution comparable to the Keck and from images enhancement by deconvolution. Still this lack of detection does not imply that there was no cloud activity at that time. This may indicate that clouds at that time were simply too small to be detected (less than 400 km), and/or optically too thin (Hirtzig et al., in preparation). Huygens/DISR also reported another occurrence of possible cloud: a thin layer was needed at 21 ± 0.5 km to reproduce the Side-Looking Imager intensity observed; Tomasko et al. (2005) suggested that it could be a layer of haze, but it could also indicate methane condensation (Tokano et al. 2006b). Indeed Lorenz et al. (2007) found at this altitude evidence of turbulence in the Huygens descent data, imputable to such a thin cloud layer. Again, the lack of thick clouds does not mean that there was no thin cloud either at the time of the observations.

[2] Shannon's principle states that a feature is reasonably real if it spans at least 2 pixels in an image. Pixel-sized features may be discarded as artefacts or cosmic rays, for instance.

4.4 Titan clouds at the north pole

Cloud activity used to be poorly constrained in the northern hemisphere, in particular close to the northern terminator and in the polar night; only the northern limb could be imaged, at ≃60°N, from Earth-based facilities. Only the Voyager and Cassini spacecraft could gather data at such high latitudes, reporting several features.

A large northern phenomenon, that we shall call from now on "north polar cloud system (NPCS)", hovers above the north pole (PIA09171) and forms an entire cap northward of 56°–62°N (PIA10511). It was discovered by Cassini/VIMS on the 29th of December 2006, and confirmed 2 weeks later, during the following Titan flyby, on the 13th January 2007: Griffith et al. (2006) reported "ethane cloud" detections at the northern terminator, like in Fig. 3 (middle panel). Rodriguez et al. (2009) confirms that since 2007, it was detected during nearly all Cassini flybys. The spectrum of this northern cloud differs from the one of the SPCS: it is visible only from 2.068 to 2.152 μm, and blends into the limb-brightening longward of 2.168 μm. Still, there may be more similarities between the north and the south pole, since Brown et al. (2009) and Rodriguez et al. (2009) could detect some convection clouds exactly like the SPCS, below the large NPCS homogeneous cap, that they call "streaks" or "knots".

Eventually, cirrus clouds were proposed by Mayo and Samuelson (2005): Voyager/IRIS had detected at 64°–77°N spectral signatures of an optically thin cloud, in the 16-50 μm range. Although no chemical identification was possible, this cloud was suggested to consist of HCN, since the winter hemisphere is supposed to have a larger supply of chemical species (Samuelson et al. 1997a). From Cassini/CIRS observation, de Kok et al. (2008) confirm that HCN may be of some importance in the creation of such cirrus clouds at ≃ 140 km of altitude, even though the chemical response of HCN may be masked by its mixing with other ices or its chemical alteration.

4.5 Short-term evolution of the clouds

Cassini images showed a fast evolution of clouds both at the south pole and at mid-latitudes (Porco et al. 2005; Griffith et al. 2005), in agreement with ground-based observations (Griffith et al. 2000; Bouchez and Brown 2005). Convective clouds on Titan seem to have a lifetime of a few hours, and, assuming the features are related to the same cloud, they move at speeds of typically a few metres per second (Porco et al. 2005),[3] values compatible with the GCM predictions (Tokano et al. 2006b).

Griffith et al. (2005) focused on a series of six VIMS datacubes acquired on 13th December 2004 (Cassini TB flyby) in a 3-h sequence. The appearance of the clouds changes as time goes by, which can be due to motion, deformation, or spatial resolution effects, but their spectral behaviour also changes. In particular, the slope of the spectrum in the 2.12–2.15 μm range increases quickly (by a dozen % in half an hour), which can be explained by an increase in cloud opacity and/or an increase in

[3] Exceptionally one cloud moved at a speed of up to 34 ± 13 m/s at 38°S latitude (Porco et al. 2005).

cloud altitude. According to Griffith et al. (2005), the features rise give from 10–14 to 40–44 km in altitude along with an opacity increase of 0.0–0.4.

Particularly interesting is one special cloud event which was observed by VIMS [cloud 2 on Fig. 3 of Griffith et al. (2005)]. The image sequence indicated that vigorous vertical evolution was followed by horizontal growth and transport at a speed of about 14 m/s. Larger features were also observed to fade out, in agreement with a fast evolution and deformation of the whole cloud system. This was explained by a drop in altitude and optical density due to rainout of millimetre-sized droplets (Toon et al. 1988; Lorenz 1993; Karkoschka and Tomasko 2009). As a conclusion, it is very plausible to consider convective plumes within the troposphere (Lorenz et al. 2005): such plumes may climb convectively, grow, and follow the wind direction. The "tail" of the plume will eventually rain out in a few hours.

Additionally, some elongated clouds curve slightly poleward from west to east (Roe et al. 2005b), which is consistent with the presence of some meridional wind in Titan's troposphere as measured by Huygens (Karkoschka et al. 2007). Similarly, the small clouds embedded within the SPCS rotate slowly around the north pole, as if they are carried by the wind (Bouchez and Brown 2005; Porco et al. 2005).

5 Extraction of cloud parameters

5.1 Radiative transfer models

Radiative transfer (RT) models are compulsory to extract from Titan's observations sensitive parameters such as cloud altitude, surface albedo or aerosol distribution by separating the surface and the atmospheric contributions. Earlier studies of the surface relied solely on a comparison between observations in the methane windows (0.83, 0.94, 1.24, 1.64, 2.0 μm) and the near-by methane bands to separate the atmosphere from the surface (Smith et al. 1996; Coustenis et al. 2001). In imagery, the RT code merely gives us access to the altitude probed by each filter in Titan's atmosphere (as on Fig. 4): the narrower the filter bandwidth, the smaller the altitude range, even though the contribution function core of such narrow-band filters still spans tens of kilometres. The use of RT codes to calculate surface albedo maps still suffers from large error bars (as we will underline later, the choice of the input parameters is critical), and only relative albedo maps can be produced. In the case of spectroscopic studies, the RT code is the very base of all the interpretation, since it is used to fully reproduce the data, from the methane windows (with assumptions on the surface spectrum) to the methane absorption bands (in the upper atmosphere).

To make comparisons, we have used a RT code to compute the altitude probed by various filters. Figure 4 shows some of the result obtained for VIMS data. Our code is an updated version of the McKay et al. (1989) one, taking into account the microphysical evolution of the fractal aerosols. We used the DISR, HASI and GCMS Huygens data as a reference for the pression, temperature and methane mixing ratio indicators, and the SHDOMPP (Evans 1998) routine as our calculator. Methane absorption is described by the Boudon et al. (2006) database for the largest part (longward of 1.6 μm), along with the Karkoschka (1998) coefficients; computation time is reduced

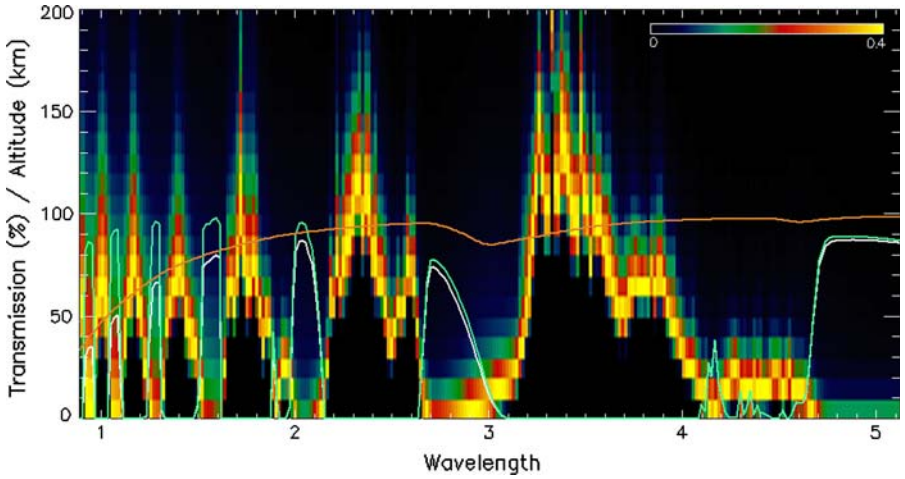

Fig. 4 Example of radiative transfer models outputs [here from the model by Rannou et al. (2006)], applied to VIMS nadir data (Hirtzig et al., in preparation). In *white*, *brown* and *cyan* are represented the transmission of Titan's atmosphere (in %) over the VIMS infrared range (0.8–5.2 µm) at the VIMS spectral resolution. The *white curve* corresponds to the transmission of the entire atmosphere, to be compared to the contribution of the pure methane (in *cyan*) or the aerosols alone (in *brown*). On the other hand, the background image represents the weight function as a function of wavelength and altitude: the percentage of atmospheric contribution is shown in colour. The methane bands and windows can easily be distinguished on the figure: the windows are optically thin (high transmission), and can probe down to the surface (apart from short wavelength filters, the atmospheric contribution is low, and focused only in the first dozens of kilometres), while the bands are optically thick and probe down to the troposphere or the stratosphere. The red–orange–yellow range corresponds to the peak of the weight function, that generally spans about 50 km in altitude. The altitude peak around 3 µm here is due to methane fluorescence that was not implemented in this particular model. Note that for other models (different aerosols and/or methane descriptions), the altitude range can be extended by $\simeq$20%

via the correlated-K method (Goody et al. 1989). Where available, the Karoschka coefficients are updated according to Irwin et al. (2006) or Tomasko et al. (2008a). Fractal aerosols are extracted from the Rannou et al. (2005) GCM results, that predicts the aerosol population based on a micro-physical and chemical model. A cutoff level is added (80 km) below which the aerosol opacity is assumed to be constant, a step compulsory though arbitrary to reproduce the data.

5.2 Uncertainties on models input parameters

Independently of the method used (two-streams or adding-doubling, to name but a few), any RT code requires at least a synthetic summary of Titan's atmospheric properties. In terms of radiative transfer, Titan's atmosphere can roughly be reduced to two main constituents, namely methane and aerosols. Indeed, nitrogen is almost transparent in the infrared, even though it represents 98% of the atmosphere: the only influence of nitrogen in RT codes can be found in the collision-induced absorption (CIA) features found at 2, 4.3 µm, and in the thermal infrared. In the K band (around 2 µm), where most clouds studies have been conducted, the influence of the H_2 CIA lines is

not negligible, but very well constrained, compared to the low-accuracy characterization of the cold long-pathlength methane absorption. Several databases are available on methane absorption: on the one hand, theoretical line-by-line work by Boudon et al. (2006), and on the other hand band models extrapolated from laboratory measurements (Karkoschka 1998; Irwin et al. 2006). Line parameters for gases of interest in atmospheric applications have been compiled in two extensive databases: the High Resolution Transmission Molecular Absorption Database (HITRAN) (Rothman et al. 2005) and the Management and Study of Atmospheric Spectroscopic Information [Gestion et Etude des Informations Spectroscopiques Atmosphériques—GEISA—of Jacquinet-Husson et al. (2005)] listings. However, the methane absorption coefficients are quite inaccurately known to this date: the theoretical work is limited to wavelengths longer than 1.6 μm (Albert et al. 2008), and only $\simeq$16% of the lines of the tetradecad (which represent $\simeq$50% of the absorption) are reproduced (V. Boudon, private communication). Furthermore, laboratory measurements are conducted at temperature–pressure conditions different from what exist on Titan. This greatly influences the results of RT modelling. Negrão et al. (2006) and Negrão (2007) showed, for instance, that the atmospheric transmission could easily vary by a factor of five from one database to another. Tomasko et al. (2005) also showed from Huygens/DISR measurements that the absorption coefficients generally used [the ones by Karkoschka (1998)] are probably overestimated by a factor of 2. This begs for an exhaustive study and eventually a consensus on the methane absorption coefficients.

The aerosols of Titan can be predicted either by one-dimensional microphysical and RT models (McKay et al. 1989) or coupled haze microphysics-dynamics models like the one by Rannou et al. (2004). In the absence of sufficient observational constraints, the first microphysical models made assumptions regarding the size, shape and density of the aerosols. For instance, Cabane et al. (1992) proposed a model where aerosols could be spherical in the upper atmosphere, and fractal at lower altitudes. This was compatible with measurements above the tropopause from stellar occultation data (Sicardy et al. 1990; Hubbard et al. 1990). But all models required a depletion in aerosols population below a cut-off altitude, something that was not observed by Huygens/DISR (Tomasko et al. 2005). Ádámkovics et al. (2007), Bar-Nun et al. (2008) and Tomasko et al. (2008b) demonstrated that improvements in the haze vertical profile can help us to reproduce both Huygens/DISR and VLT/SINFONI observations.

The uncertainties on the methane absorption coefficents are a major drawback in the altitude computation, because aerosols are negligible in this calculation: they merely influence the contrast of the image and the retrieval of parameters like cloud opacity. In any case, RT models considerably vary from each other (algorithms, absorption databases, and so on) that we cannot be more precise than a dozen kilometers when defining the levels probed by the filters. Thus we can only differentiate four types of filters: surface ones (0–10 km main contribution) in the core of the methane windows, tropospheric ones (0–40 km) in the weak methane wings, tropopause ones (20–60 km) in the strong methane wings, and stratospheric ones (40–300 km) in the methane bands. It is also worth remembering that filters will probe atmospheric levels some 20 km higher on Titan's limb than in the main part of the disk (nadir observations for in situ measurements).

5.3 Altitude of the clouds

Three methods can be used to retrieve the clouds altitudes: (1) direct modelling (the only method possible for interpreting spectroscopic data), (2) altitude comparisons between filters where the feature is respectively visible or invisible (this also requires modelling as in Fig. 4) and (3) cloud tracking.

Brown et al. (2002) rely on radiative transfer modelling of the Keck 2-μm spectra, placing a highly reflective cloud layer at an altitude of 16 ± 5 km; such computations led Porco et al. (2005) to suggest that the cloud top could be as high as ≃25 km. Cassini/VIMS and spatially-resolved spectroscopy provide us with more specific information: the SPCS is visible with much more detail than from the Earth in nearly all the wings of the methane windows (with ISS and VIMS) but it is also recognizable by its spectral signature: broadening of the 2.0, 2.8, and 5 μm windows, as well as enhancement of the 4 and 4.5 μm narrow windows, like any other cloud. As explained in Griffith et al. (1991), the larger the broadening, the higher the cloud; conversely, the steeper the slope, the lower the cloud (Griffith et al. 2005). In Fig. 3, the example of the 40°S cloud spectrum can be explained by a cloud thinner and/or lower than the SPCS. However, in general, there is no significant difference in altitude between the SPCS, the mid-latitude clouds spectra, and the small "knots" below the NPCS, apart from the overall brightness.

The second method was used in Hirtzig et al. (2006) for the SPCS, assuming that it was necessarily below the altitude probed by the NB_2.17 VLT/NACO filter (2.166 ± 0.010 μm) (where the feature was invisible). This is a strong constraint, but the computation of the altitude probed by each filter is very model-dependent, as is the calculation of the contribution function for these filters. The altitude given in Hirtzig et al. (2006) is 17–83 km, more probably 17–40 km. In Roe et al. (2002a) the clouds are not seen in the Brackettγ (2.17 ± 0.010 μm) filter, indicating that the clouds are located below 50 km in the troposphere (Roe et al. 2002a; Bouchez and Brown 2005). Cassini/ISS data might provide us with further constraints since the SPCS is scarcely detectable in the MT1 (0.619 μm) filter, while the other mid-latitude clouds are invisible at this wavelength, indicating that these clouds may exist at lower altitudes and/or are less bright than the SPCS. VIMS data confirm this (Fig. 3), and altitude values returned are of the same order as the 16–27 km inferred for unresolved clouds in Griffith et al. (2000).

Bouchez and Brown (2005) propose another method to determine the SPCS altitude: tracking the motion of the clouds detected during several successive nights may lead to a rough estimate of the wind speed; in fact, no clear motion could be measured from the Earth, leading to an upper limit of a few metres per second. Similarly, the tracking of two of the ISS streaks led to speed estimates lower than 10 m/s (Porco et al. 2005). This wind speed is consistent with the in situ wind measurement by Huygens (Folkner et al. 2006). This may indicate that the clouds are at low altitudes, probably lower than 40 km, even though the speed of the cloud particles can largely differ from the speed of the cloud itself (like orographic clouds which stuck to a mountain while their particles continue to drift with the wind). Cassini proved, however, that the SPCS was dissipating faster than it moved, and the speed measurements may in fact wrongly be interpreting this fast deformation as a real motion.

We propose here to apply these methods to estimate the altitude of all the other phenomena listed previously. If possible, we need to focus only on a small wavelength range to assume that there is no spectral change in the response of the haze, methane, and the feature itself. Otherwise, we have to rely on assumptions regarding the feature's chemical constituents or particle size to compensate for the possible lack of constraints. To simplify, we assume that the brightness of aerosol particles decreases in the 1–2 μm range (Coll et al. 2003; Roush and Dalton 2004; Bernard et al. 2006), while ethane condensates are bright longward of 2 μm, and methane condensates are bright at all wavelengths.

5.3.1 Southern polar collar

In the I–J bands, we can locate a feature similar to a polar collar around the southern tropopause. Indeed, the main contribution of 1.04, 1.09, and 1.24 μm filters comes from the tropopause, where the feature is brightest. The same demonstration can be applied separately in the H and K bands: from the H band images, the feature is located in or below the lower stratosphere, and in the K band it can be found faintly at low altitudes, and disappears completely in the stratosphere. The most plausible explanation tends to suggest that all these different features are located around the tropopause.

Brown et al. (2002) incorporate the "tropopause cirrus" in their RT model as an optically thin (optical depth of 0.10 ± 0.02 at 2 μm) layer at 30–40 km of altitude, while Roe et al. (2002b) locate the southern "collar" above 40–50 km. Bouchez (2003) located a bright scattering region near the south pole at an altitude of 35 ± 10 km, citing possible cirrus-like, optically thin methane condensation clouds. So all observers tend to set this feature near the tropopause. It is thus highly plausible that the "serpentine feature", the polar "collar", and the "tropopause cirrus" all correspond to the same feature. The same conclusion can be made regarding the SPCS companions.

5.3.2 Ethane cloud

Figure 3 (middle panel) shows that the brightness of the limb is not what would usually be expected without a cloud (as in the upper panel): the limb-brightning is usually obvious only longward of 2.168 μm, but in this case, the limb is already very bright from 2.068 to 2.152 μm, because of the ethane cloud. This leads to an altitude of the feature between 30 and 60 km, more probably around 40 km assuming the regular limb-brightening takes precedence at 2.168 μm, an altitude somewhat higher than the 16–27 km inferred for unresolved clouds in Griffith et al. (2000).

5.3.3 Northern cap

This feature is bright on the H1702 images, and invisible on the J1158 ones. From the Keck data interpretation, the J1158 filter probes down to 90 km, while the H1702 one probes down to 20–30 km. A similar feature can be detected faintly on one 1.64 μm VLT image in Gendron et al. (2004), with a wide filter probing from the surface to the tropopause. If this faint feature is related to this phenomenon, then we can definitely

constrain this "northern cap" to lie in the lower part of the H1702 filter altitude range, probably between 20 and 60 km.

Since this feature does not appear on the J1158, we can combine constraints on both its spectral behaviour and its altitude. If the component is equally bright in the H and J bands (for instance what we expect from methane clouds), then the feature must lie at low altitude, between 20–30 and 90 km altitude, far from the J1158 filter probing range (for this filter, opacity reaches unity at 90 km, which does not forbid a small contribution from lower levels). If the component is brighter in the J band, then it must lie at even lower altitude not to be detected on the J1158 image, in the lowest part of the 20–90 km range deduced previously. Eventually, if the component is darker in the J band (specific material with a brightness peak around 1.7 μm, as well as 2- μm-sized droplets or bigger), then we do not have any upper limit on the altitude. The dark feature would blend seamlessly into the limb-darkening observed in the J1158 images.

To date, no other data can corroborate this. The ethane cloud can be an explanation of this northern cap: ethane particles are indeed brighter at 1.7 than at 1.1 μm. Similarly, this northern cap could be a reminiscent of the cirrus clouds proposed by Mayo and Samuelson (2005): Voyager/IRIS had detected an optically thin cloud at 64°–77°N. Mayo and Samuelson (2005) modelled a cirrus cloud of 1–5 μm at 58–90 km of altitude, assuming HCN as a component since it can condense at 90 km and produce particles of 3–4 μm. Again, such particles would be indeed darker in J band than in H band, compatibly with Roe et al. (2002a) observations.

Eventually, GCMs investigate the layers of haze at the north pole (Rannou et al. 2004; Strobel 2006; Walterscheid and Schubert 2006), but they lay at altitudes around 200 km, which is not consistent with the observations analysed here. As a conclusion, we do not know exactly where or what this "northern cap" may be: it is either at lower altitudes than the "tropopause cirrus" and presumably made of CH_4, or composed of particles bigger than 2 μm (possibly HCN or C_2H_6).

5.3.4 Morning stratospheric haze enhancement

Inferring the altitude of this phenomenon is the first step to understand its nature. It seems to be around 70–90 km (Coustenis et al. 2001), or rather around 80–120 km (Hirtzig et al. 2006). This is compatible with the 70–90 km altitude predicted by the GCMs (Rannou et al. 2003). Models need to be developed to describe this phenomenon: the night in the upper atmosphere of Titan does not last 8 Earth days, because the super-rotation of Titan's atmosphere imposes a speed of about 100 m/s at about 100 km of altitude (Luz et al. 2005; Kostiuk et al. 2001), thus a particle carried by the wind would stay in Titan's shadow for only some 20 h. Only models on the physical properties of the aerosols (based on their laboratory analogues, the tholins) can solve this problem, since we cannot choose between the two options: tiny but sticky particles drifting with the wind, or larger particles less sensitive to the wind which could spend more time in Titan's night. This explanation is only valid for cloud features detected in the stratosphere, and obviously only near the morning limb or terminator.

6 Discussion

6.1 The nature of Titan clouds

From Cassini/VIMS and near-infrared Cassini/ISS data we know that all the tropospheric clouds are bright at least from 0.9 to 5 μm, compatible with the expected behaviour of methane particles exceeding 5 μm in size. In this case, the VIMS elongated clouds would appear bright also in the visible, exactly like the ISS "zonal streaks", which supports our suspicion that both phenomena were the same. The altitude of the unresolved clouds reported by Griffith et al. (2000) (16–27 km) is also compatible with the ones estimated for these clouds (20 ± 10 km). Barth and Toon (2006) model the formation of cloud particles, and show that methane can condensate onto bare and ethane-coated aerosols between 0 and 30 km, producing 10–100-μm-sized particles near the top of the cloud, up to millimetre size close to the surface where the droplets rain out.

The thin bright collar located along the 70°S parallel at 30 ± 10 km may reconcile with the different observations of a "serpentine feature" (Hirtzig et al. 2007), a polar "collar" (Roe et al. 2002a), and the "tropopause cirrus" (Brown et al. 2002); Table 2 shows that the southern features are bright at short wavelengths (at 1.04 and 1.09 μm), but become fainter at longer wavelengths. Such an indication may be pointing at aerosols as the main constituents of this feature since the haze is optically thicker in the near infrared than at longer wavelengths (Khare et al. 1984). The two companions of the SPCS spotted by Hirtzig et al. (2006) have the same behaviour in K band as this "tropopause cirrus". It is thus plausible to assume that they are, in the order of ascending credibility:

- Northern delimitation of a stratospheric hood of haze swept away from the equator by atmospheric dynamics (Rannou et al. 2002, 2004), artificially enhanced by deconvolution (in particular on the Gibb's ring). Such a hood would probably lie at higher altitudes than the ones estimated by the Keck team (30 ± 10 km).
- Real clouds: higher in altitude with respect to other cloud detections (although mid-latitude elongated clouds are reported at similar latitudes, they lay at slightly lower altitudes than the SPCS); they are motionless from one observation to another, attached to Titan's limb [while the SPCS is slightly moving on the CFHT and VLT images, as are Roe et al. (2005a) "transient clouds"].
- Another appearance of the "tropopause cirrus", enhanced on the limbs by the Gibb's ring.

As mentioned before, the ethane cloud (probably the NPCS seen side-on) is located above Titan's northern limb, between 30 and 60 km of altitude, where the peak of aerosols distribution is expected according to GCM (general circulation model) predictions (Rannou et al. 2006). Since this feature is not very bright at short wavelengths, the authors infer that the particles therein must be larger than 1 μm in size; similarly, the cloud is thin at $\lambda \simeq 5$ μm, inducing particle size smaller than 3 μm. Only ethane particles can be that small: methane particles such as the ones expected within the SPCS clouds would reach tens of microns (Toon et al. 1988). Furthermore, the altitude of the clouds (40–65 km) is too high for methane condensation, but not for ethane clouds (Sagan and Thompson 1984; Barth and Toon 2003; Bauerecker and Dartois 2009).

Indeed the Barth and Toon (2006) cloud microphysics model predicts ethane condensation onto tholins at 30–40 km, with typical sizes around 1–10 μm (significantly smaller than methane particles). Eventually, Rannou et al. (2006) GCM predicts clouds at low northern latitudes, around 40°N, but none were observed to date (Rodriguez et al. 2009).

6.2 Formation mechanisms of Titan's clouds

Several theories have been put forward in the last decade to explain the clouds formation. They are by no mean exclusive, and can complement each other, as we will show.

6.2.1 The SPCS

- Clouds may form when the atmosphere, usually devoid of cloud condensation nuclei, is enriched by the downwelling of ethane ice from the cold stratospheric spring pole (Samuelson and Mayo 1997; Roe et al. 2002b).
- Cloud formation may also be induced by the heating of the surface by solar insolation, driving the cloud activity in correlation with the seasonal cycle of insolation (Brown et al. 2002; Tokano 2005; Mitchell et al. 2006). Still, this theory could explain the disappearance of the SPCS in 2005 (Schaller et al. 2005, 2006a; Rodriguez et al. 2009), but neither its weak reappearance in 2006 nor its probable presence as early as 1996–1998 (Gibbard et al. 2004a).
- According to the GCM by Rannou et al. (2006), the clouds may be trapped into the remnant Hadley cell at the south pole, ascending moist air into the colder mid-troposphere. Indeed their model predicts most of the clouds locations (at the pole and at the tropics), making a strong case that cloud formation may be driven by large-scale circulation.
- Locally, clouds may form if the atmosphere is moist enough: Hueso and Sánchez-Lavega (2006) and Barth and Rafkin (2007) showed that a small temperature variation could trigger moist convection, in case of a high methane concentration. Mitri et al. (2007), Brown et al. (2009), and Lunine and Atreya (2008) proposed the evaporation of the lakes material as a plausible source for locally high moisture; a recent ISS study showed that lakes may be more numerous at the south pole than expected (Turtle et al. 2009), complementing the northern lakes (Stofan et al. 2007) and confirming that liquid methane seasonally accumulates near both poles (Stevenson and Potter 1986).
- Eventually, cloud formation may be linked to large-scale planetary waves. In Luz and Hourdin (2003), Barth and Toon (2004) and Tokano (2008a) modelled the temperature fluctuations and the tidal wind variations due to such waves, which may both encourage the formation of convective features.

6.2.2 Mid-latitude clouds

Generally speaking, these convective clouds (Griffith et al. 2005) are compatible with the moist convection models by Hueso and Sánchez-Lavega (2006) and

Barth and Toon (2006), and with the GCM predictions by Rannou et al. (2006). Griffith et al. (2008) suggest that the atmosphere is neither wet nor warm enough to trigger cloud condensation at the tropics: in this case, only the horizontal mixing due to inertial instability may explain the presence of clouds at such specific latitude ($\simeq$40°S), in the ascending branch of the Hadley circulation.

On the other hand, if the geographical control suggested by Roe et al. (2005b) is proven [Rodriguez et al. (2009) conclusions favour a tidal control], then orographic sources could be found: cryovolcanic activity or geysers may be the most plausible triggers.

6.2.3 Stratiform clouds

These optically thin clouds could produce some drizzle in Titan's atmosphere (Tokano et al. 2006b; Ádámkovics et al. 2007). They are reproduced by Barth and Rafkin (2007) with their moist convection model, in cases when the methane humidity is not high enough to trigger convection (and then flocky clouds). Tokano et al. (2006b) suggested that this type of cloud may be caused by slow upward motion as part of the global Hadley circulation. But the drizzle itself remains to be proved, as Kim et al. (2008) underline.

6.2.4 NPCS

The clouds at the north pole fall into two categories: the "ethane cloud" at the tropopause (Griffith et al. 2005), and the possible "lake-effect clouds" (Brown et al. 2009). The former are related to both the large-scale circulation (Rannou et al. 2006) and the downwelling of aerosols and ethane within the polar night (Samuelson and Mayo 1997), that drags upper atmosphere species into the lower atmosphere (Coustenis and Bezard 1995; Coustenis et al. 2007), similarly to what happens in the middle atmosphere on Earth (Andrews et al. 1987; Abrams et al. 1996a,b). The latter "lake-effect clouds", on the other hand, are examples of moist convection in a locally wet environment (Hueso and Sánchez-Lavega 2006; Barth and Rafkin 2007; Mitri et al. 2007; Brown et al. 2009).

7 Conclusions

In this paper we presented an overview of the cloud observations between 1993 and 2008, as well as other diurnal and seasonal phenomena. Nowadays, Global Circulation Models reproduce fairly well the evolution of the north–south asymmetry ruled by the seasonal evolution of the aerosols population. Diurnal effects, such as the nocturnal condensation occurring in the stratosphere, can theoretically be modelled, but they are not included in the most recent GCMs. Titan's clouds have been thoroughly monitored, and theoretical models have gradually revealed their nature.

Two different types of clouds have been observed: the first type of clouds comprises flocky, quickly evolving clouds, resembling convective plumes, either in a larger group of clouds (SPCS) or single features above given parallels ("transient clouds" and "zonal

streaks" at 40°S), at 20 ± 10 km of altitude; the latter clouds seem to be lower and/or thinner than the clouds within the SPCS.

The second type of clouds are cirrus-like clouds at higher altitudes. The "tropopause cirrus" and "ethane clouds" are optically thinner than the flocky clouds, and are observed at various altitudes, higher than the SPCS, roughly between 20 and 90 km. The former is certainly related to haze (as established in Sect. 6.1), while the latter, at 30–60 km altitude, is probably made of 1–3 μm large ethane condensates. Elongated clouds at ≃40°N may also be related to the southern extent of the north pole haze cap. Condensation of HCN at around 90 km is also plausible.

Thermodynamics and atmospheric dynamics seem to rule the nature of the features detected in Titan's atmosphere: at 20 ± 10 km of altitude, the SPCS and mid-latitude clouds can be convective plumes of methane, possibly associated to lakes, or non-convective clouds caused by large-scale circulation. At higher altitude, only ethane can condense (the "ethane cloud" detected by Griffith et al. (2006) at 30–60 km at the northern terminator as well as the NPCS).

Several hypotheses have been put forth to explain the formation of the low-altitude clouds such as spring pole condensation, insolation-driven moist convection, large-scale transport of moist air into the cold polar region or moist convection triggered by a local methane source. Some of the mechanisms conflict with each other and observations of clouds alone may not be sufficient to fully understand the cloud formation. Temperature, methane humidity and wind data in the troposphere are required and possible methane sources on the surface have to be searched for.

In the future, efforts should also be made in the investigation as to whether the various clouds observed are driven by similar phenomena or not. In any case, this is a compulsory step towards a better understanding of how the methane hydrological cycle works on Titan.

All these observations provide the scientific community with constraints on the atmospheric dynamics. In the future, the comparison of data from various techniques, during joint missions of observations will provide the community with a stronger set of time constraints on the atmospheric dynamics. Simultaneously, the improvement of RT models, via a better knowledge of the methane spectrum, while GCM will eventually reproduce and predict the seasonal, diurnal, and short-term phenomena linked with the aerial part of Titan's methane cycle.

Acknowledgments The authors want to thank Caitlin A. Griffith and Athena Coustenis for fruitful discussions. The constructive comments made by Thérèse Encrenaz and an anonymous referee were also greatly appreciated. Tetsuya Tokano was supported by DFG.

References

Abrams MC et al (1996a) ATMOS/ATLAS-3 observations of long-lived tracers and descent in the Antarctic vortex in November 1994. Geophys Res Lett 23:2341–2344. doi:10.1029/96GL00705

Abrams MC et al (1996b) Trace gas transport in the Arctic vortex inferred from ATMOS ATLAS-2 observations during April 1993. Geophys Res Lett 23:2345–2348. doi:10.1029/96GL00704

Ádámkovics M, de Pater I, Hartung M, Eisenhauer F, Genezl R, Griffith CA (2005) The 3-dimensionnal distribution of Titan haze from near-infrared integral field spectroscopy. J Geophys Res

Ádámkovics M, Wong MH, Laver C, de Pater I (2007) Widespread morning drizzle on Titan. Science 318:962–965. doi:10.1126/science.1146244

Albert S, Bauerecker S, Boudon V, Brown L, Champion J-P, Lote M, Nikitin A, Quack M (2008) Global analysis of the high resolution infrared spectrum of methane $^{12}CH_4$ in the region from 0 to 4800 cm-1. Chem Phys (in Press). Corrected proof. doi:10.1016/j.chemphys.2008.10.019

Anderson CM, Chanover NJ, McKay CP, Rannou P, Glenar DA, Hillman JJ (2004) Titan's haze structure in 1999 from spatially-resolved narrowband imaging surrounding the 0.94 μm methane window. Geophys Res Lett 31:17

Anderson CM, Young EF, Chanover NJ, McKay CP (2008) HST spectral imaging of Titan's haze and methane profile between 0.6 and 1 μm during the 2000 opposition. Icarus 194:721–745. doi:10.1016/j.icarus.2007.11.008.

Andrews DG, Holton JR, Leovy CB (1987) Middle atmosphere dynamics. In: Andrews DG, Holton JR, Leovy CB (eds) Middle atmosphere dynamics. Academic Press, New York, pp 489, Price US $34.95

Babcock HW (1953) The possibility of compensating astronomical seeing. Publ Astron Soc Pac 65:229–236

Baines KH et al (2005) The atmospheres of Saturn and Titan in the near-infrared first results of Cassini/vims. Earth Moon Planets 96:119–147. doi:10.1007/s11038-005-9058-2

Bar-Nun A, Dimitrov V, Tomasko M (2008) Titan's aerosols: comparison between our model and DISR findings. Planet Space Sci 56:708–714. doi:10.1016/j.pss.2007.11.014

Barth EL, Rafkin SCR (2007) TRAMS: a new dynamic cloud model for Titan's methane clouds. Geophys Res Lett 34:3203. doi:10.1029/2006GL028652

Barth EL, Toon OB (2003) Microphysical modeling of ethane ice clouds in titan's atmosphere. Icarus 162:94–113

Barth EL, Toon OB (2004) Properties of methane clouds on Titan: results from microphysical modeling. Geophys Res Lett 31:17

Barth EL, Toon OB (2006) Methane, ethane, and mixed clouds in Titan's atmosphere: properties derived from microphysical modeling. Icarus 182:230–250. doi:10.1016/j.icarus.2005.12.017

Bauerecker S, Dartois E (2009) Ethane aerosol phase evolution in Titan's atmosphere. Icarus 199:564–567. doi:10.1016/j.icarus.2008.09.014

Bernard J-M et al (2006) Reflectance spectra and chemical structure of Titan's tholins: application to the analysis of Cassini Huygens observations. Icarus 185:301–307. doi:10.1016/j.icarus.2006.06.004

Bouchez AH (2003) Seasonal trends in Titan's atmosphere: haze, wind, and clouds, Ph.D. Thesis

Bouchez AH, Brown ME (2005) Statistics of Titan's south polar tropospheric clouds. Astrophys J 618:L53–L56

Boudon V, Rey M, Loete M (2006) The vibrational levels of methane obtained from analyses of high-resolution spectra. J Quant Spectrosc Radiat Transf 98:394–404

Bratsolis E, Sigelle M (2001) A spatial regularization method preserving local photometry for Richardson-Lucy restoration. Astron Astrophys 375:1120–1128

Brown ME (2005) The seasonal hydrological cycle on Titan. In: Proceedings of the conference "Titan after the Huygens and First Cassini Encounters", Crete, Greece, 30 May–3 June 2005. http://www.lpl.arizona.edu/titanconference/index.html

Brown ME (2000) The solar system up close: AO spectroscopy from Palomar. Bull Am Astron Soc 32:1508

Brown ME, Bouchez AH, Griffith CA (2002) Direct detection of variable tropospheric clouds near Titan's south pole. Nature 420:795–797

Brown ME, Schaller EL, Roe HG, Chen C, Roberts J, Brown RH, Baines KH, Clark RN (2009) Discovery of lake-effect clouds on Titan. Geophys Res Lett 36:1103. doi:10.1029/2008GL035964

Brown RH et al (2006) Observations in the Saturn system during approach and orbital insertion, with Cassini's Visual and Infrared Mapping Spectrometer (VIMS). Astron Astrophys 446:707–716. doi:10.1051/0004-6361:20053054

Cabane M, Chassefiere E, Israel G (1992) Formation and growth of photochemical aerosols in Titan's atmosphere. Icarus 96:176–189

Caldwell J et al (1992) Titan: evidence for seasonal change—a comparison of hubble Space telescope and voyager images. Icarus 97:1–9

Chanover NJ, Anderson CM, McKay CP, Rannou P, Glenar DA, Hillman JJ, Blass WE (2003) Probing Titan's lower atmosphere with acousto-optic tuning. Icarus 163:150–163

Coll P, Jolly A, Bernard J-M, Ramirez SI, da Silva A, Navarro-Gonzalez R, Lafait J, Rannou P, Raulin F (2003) Optical properties of Titan's aerosol analogues (in the 200 nm–2.5 μm range). In: EGS–AGU–EUG Joint Assembly, Abstracts from the meeting held in Nice, France, 6–11 April 2003, abstract #12426, pp 12,426

Combes M, Vapillon L, Gendron E, Coustenis A, Lai O, Wittemberg R, Sirdey R (1997) Spatially resolved images of Titan by means of adaptive optics. Icarus 129:482–497
Conan JM, Fusco T, Mugnier L, Kesralé E, Michau V (1998) Deconvolution of adaptive optics images with imprecise knowledge of the point spread function: results on astronomical objects. In: Astronomy with adaptive optics: present results and future programs, ESO/OSA Workshop, September 1998, Sonthofen, Germany
Courtin R (1982) The spectrum of Titan in the far-infrared and microwave regions. Icarus 51:466–475
Courtin R, Gautier D, McKay CP (1995) Titan's thermal emission spectrum: reanalysis of the Voyager infrared measurements. Icarus 114:144–162
Coustenis A, Bezard B (1995) Titan's atmosphere from Voyager infrared observations. 4: latitudinal variations of temperature and composition. Icarus 115:126–140
Coustenis A, Lellouch E, Maillard JP, McKay CP (1995) Titan's surface: composition and variability from the near-infrared albedo. Icarus 118:87–104
Coustenis A, Hirtzig M, Gendron E, Drossart P, Lai O, Combes M, Negrão A (2005) Maps of Titan's surface from 1 to 2.5 μm. Icarus 177:89–105. doi:10.1016/j.icarus.2005.03.012
Coustenis A et al (2001) Images of Titan at 1.3 and 1.6 μm with Adaptive optics at the CFHT. Icarus 154:501–515
Coustenis A et al (2007) The composition of Titan's stratosphere from Cassini/CIRS mid-infrared spectra. Icarus 189:35–62. doi:10.1016/j.icarus.2006.12.022
Crespin A, Lebonnois S, Vinatier S, Bézard B, Coustenis A, Teanby NA, Achterberg RK, Rannou P, Hourdin F (2008) Diagnostics of Titan's stratospheric dynamics using Cassini/CIRS data and the 2-dimensional IPSL circulation model. Icarus 197:556–571. doi:10.1016/j.icarus.2008.05.010
de Kok R, Irwin PGJ, Teanby NA (2008) Condensation in Titan's stratosphere during polar winter. Icarus 197:572–578. doi:10.1016/j.icarus.2008.05.024
de Pater I et al (2005) Keck observations of Titan during probe entry and during the days following touchdown. In: EUROPLANET N3 activity Kick-off meeting, Graz, 8 March. http://europlanet.oeaw.ac.at/N3_Meeting_09032005.html
de Pater I, Ádámkovics M, Bouchez AH, Brown ME, Gibbard SG, Marchis F, Roe HG, Schaller EL, Young E (2006) Titan imagery with Keck adaptive optics during and after probe entry. J Geophys Res (Planets) 111:7. doi:10.1029/2005JE002620
Evans KF (1998) The spherical harmonics discrete ordinate method for three-dimensional atmospheric radiative transfer. J Atmos Sci 55:429–446. doi:10.1175/1520-0469(1998)055
Fink U, Larson HP (1979) The infrared spectra of Uranus, Neptune, and Titan from 0.8 to 2.5 microns. Astrophys J 233:1021–1040
Flasar FM (1983) Oceans on Titan? Science 221:55–57
Flasar FM (1998a) The dynamic meteorology of Titan. Planet Space Sci 46:1125–1147
Flasar FM (1998b) The composition of Titan atmosphere: a meteorological perspective. Planet Space Sci 46:1109–1124
Flasar FM, Achterberg RK (2008) The structure and dynamics of Titan's middle atmosphere. Philos Trans R Soc A Math Phys Eng Sci 367(1889):649–664. doi:10.1098/rsta.2008.0242
Flasar FM, Conrath BJ (1990) Titan's stratospheric temperatures–a case for dynamical inertia? Icarus 85:346–354
Flasar FM, Samuelson RE, Conrath BJ (1981) Titan's atmosphere–temperature and dynamics. Nature 292:693–698
Folkner WM et al (2006) Winds on Titan from ground-based tracking of the Huygens probe. J Geophys Res (Planets) 111:7. doi:10.1029/2005JE002649
Gendron E et al (2004) VLT/NACO adaptive optics imaging of Titan. Astron Astrophys 417:L21–L24
Gibbard SG, Macintosh B, Gavel D, Max CE, de Pater I, Ghez AM, Young EF, McKay CP (1999) Titan: high-resolution speckle images from the keck telescope. Icarus 139:189–201
Gibbard SG, de Pater I, Macintosh BA, Grossman A, Adamkovics M (2003) Spatially-resolved 2 micron spectroscopy of Titan from the W.M. Keck telescope. In: AAS/Division for Planetary Sciences Meeting Abstracts 35
Gibbard SG, de Pater I, Macintosh BA, Roe HG, Max CE, Young EF, McKay CP (2004a) Titan's 2 μm surface albedo and haze optical depth in 1996–2004. Geophys Res Lett 31:17
Gibbard SG, Macintosh B, Gavel D, Max CE, de Pater I, Roe HG, Ghez AM, Young EF, McKay CP (2004b) Speckle imaging of Titan at 2 microns: surface albedo, haze optical depth, and tropospheric clouds 1996–1998. Icarus 169:429–439

Goody R, West R, Chen L, Crisp D (1989) The correlated-k method for radiation calculations in nonhomogeneous atmospheres. J Quant Spectrosc Radiat Transf 42:539–550. doi:10.1016/0022-4073(89)90044-7

Griffith CA, Owen T, Wagener R (1991) Titan's surface and troposphere, investigated with ground-based, near-infrared observations. Icarus 93:362–378

Griffith CA, Owen T, Miller GA, Geballe T (1998) Transient clouds in Titan's lower atmosphere. Nature 395:575–578

Griffith CA, Hall JL, Geballe TR (2000) Detection of daily clouds on Titan. Science 290:509–513

Griffith CA, Owen T, Geballe TR, Rayner J, Rannou P (2003) Evidence for the exposure of water ice on Titan's surface. Science 300:628–630

Griffith CA, McKay CP, Ferri F (2008) Titan's tropical storms in an evolving atmosphere. Astrophys J Lett 687:L41–L44. doi:10.1086/593117

Griffith CA et al (2005) The evolution of Titan's mid-latitude clouds. Science 310:474–477. doi:10.1126/science.1117702

Griffith CA et al (2006) Evidence for a polar ethane cloud on Titan. Science 313:1620–1622. doi:10.1126/science.1128245

Hinson DP (1983) Radio scintillations observed during atmospheric occultations of Voyager: internal gravity waves at Titan and magnetic field orientations at Jupiter and Saturn, Ph.D. Thesis

Hirtzig M (2005) Etude de Titan dans l'Infrarouge Proche par Spectro-Imagerie couplée à l'Optique Adaptative, Ph.D. Thesis

Hirtzig M, Coustenis A, Lai O, Emsellem E, Pecontal-Rousset A, Rannou P, Negrão A, Schmitt B (2005) Near-infrared study of Titan's resolved disk in spectro-imaging with CFHT/OASIS. Planet Space Sci 53:535–556. doi:10.1016/j.pss.2004.08.006

Hirtzig M, Coustenis A, Gendron E, Drossart P, Hartung M, Negrão A, Rannou P, Combes M (2007) Titan: Atmospheric and surface features as observed with nasmyth adaptive optics system near-infrared imager and spectrograph at the time of the Huygens mission. J Geophys Res (Planets) 112:2. doi:10.1029/2005JE002650

Hirtzig M et al (2006) Monitoring atmospheric phenomena on Titan. Astron Astrophys 456:761–774. doi:10.1051/0004-6361:20053381

Hourdin F, Talagrand O, Sadourny R, Courtin R, Gautier D, McKay CP (1995) Numerical simulation of the general circulation of the atmosphere of Titan. Icarus 117:358–374

Hourdin F, Lebonnois S, Luz D, Rannou P (2004) Titan's stratospheric composition driven by condensation and dynamics. J Geophys Res (Planets) 109(E18):12,005

Hubbard WB, Hunten DM, Reitsema HJ, Brosch N, Nevo Y, Carreira E, Rossi F, Wasserman LH (1990) Results for Titan's atmosphere from its occultation of 28 Sagittarii. Nature 343:353–355

Hubbard WB et al (1993) The occultation of 28 SGR by Titan. Astron Astrophys 269:541–563

Hueso R, Sánchez-Lavega A (2006) Methane storms on Saturn's moon Titan. Nature 442:428–431. doi:10.1038/nature04933

Hunten DM, Tomasko MG, Flasar FM, Samuelson RE, Strobel DF, Stevenson DJ (1984) Titan, pp 671–759, Saturn

Hutzell WT, McKay CP, Toon OB (1993) Effects of time-varying haze production on Titan's geometric albedo. Icarus 105:162–174

Hutzell WT, McKay CP, Toon OB, Hourdin F (1996) Simulations of Titan's brightness by a two-dimensional haze model. Icarus 119:112–129

Irwin PGJ, Sromovsky LA, Strong EK, Sihra K, Teanby NA, Bowles N, Calcutt SB, Remedios JJ (2006) Improved near-infrared methane band models and k-distribution parameters from 2000 to 9500 cm^1 and implications for interpretation of outer planet spectra. Icarus 181:309–319. doi:10.1016/j.icarus.2005.11.003

Jacquinet-Husson N et al (2005) The 2003 edition of the GEISA/IASI spectroscopic database. J Quant Spectrosc Radiat Transf 95:429–467

Karkoschka E (1998) Methane, ammonia, and temperature measurements of the jovian planets and Titan from CCD-spectrophotometry. Icarus 133:134–146

Karkoschka E, Tomasko MG (2009) Rain and dewdrops on titan based on in situ imaging. Icarus 199:442–448. doi:10.1016/j.icarus.2008.09.020

Karkoschka E, Tomasko MG, Doose LR, See C, McFarlane EA, Schröder SE, Rizk B (2007) DISR imaging and the geometry of the descent of the Huygens probe within Titan's atmosphere. Planet Space Sci 55:1896–1935. doi:10.1016/j.pss.2007.04.019

Khare BN et al (1984) The organic aerosols of Titan. Advances in Space Research 4:59–68
Kim SJ, Trafton LM, Geballe TR (2008) No evidence of morning or large-scale drizzle on Titan. Astrophys J Lett 679:L53–L56. doi:10.1086/588839
Kondo K, Ichioka Y, Suzuki T (1977) Image restoration by Wiener filtering in the presence of signal-dependant noise. Appl Opt 16:2554–2558
Kostiuk T, Fast KE, Livengood TA, Hewagama T, Goldstein JJ, Espenak F, Buhl D (2001) Direct measurement of winds of Titan. Geophys Res Lett 28:2361–2364
Kostiuk T et al (2005) Titan's stratospheric zonal wind, temperature, and ethane abundance a year prior to Huygens insertion. Geophys Res Lett 32:22,205. doi:10.1029/2005GL023897
Kostiuk T et al (2006) Stratospheric global winds on Titan at the time of Huygens descent. J Geophys Res (Planets) 111:7. doi:10.1029/2005JE002630
Kuiper GP (1944) Titan: a satellite with an atmosphere. Astrophys J 100:378
Labeyrie A (1970) Attainment of diffraction limited resolution in large telescopes by Fourier analysing speckle patterns in Star Images. Astron Astrophys 6:85
Lebonnois S, Toublanc D, Hourdin F, Rannou P (2001) Seasonal variations of Titan's atmospheric composition. Icarus 152:384–406
Lebonnois S, Hourdin F, Rannou P, Luz D, Toublanc D (2003) Impact of the seasonal variations of composition on the temperature field of Titan's stratosphere. Icarus 163:164–174
Lellouch E, Coustenis A, Gautier D, Raulin F, Dubouloz N, Frere C (1989) Titan's atmosphere and hypothesized ocean—a reanalysis of the Voyager 1 radio-occultation and IRIS 7.7-micron data. Icarus 79:328–349
Lemmon MT, Karkoschka E, Tomasko M (1993) Titan's rotation—surface feature observed. Icarus 103:329–332
Lemmon MT, Karkoschka E, Tomasko M (1995) Titan's rotational light-curve. Icarus 113:27–38
Lindal GF, Wood GE, Hotz HB, Sweetnam DN, Eshleman VR, Tyler GL (1983) The atmosphere of Titan—an analysis of the Voyager 1 radio occultation measurements. Icarus 53:348–363
Lockwood GW, Lutz BL, Thompson DT (1979) Spectrophotometry of temporal and spatial variations of the atmospheres of the outer planets and Titan. Bull Am Astron Soc 11:554
Lorenz RD (1993) The life, death and afterlife of a raindrop on Titan. Planet Space Sci 41:647–655
Lorenz RD (2002) Thermodynamics of geysers: application to Titan. Icarus 156:176–183
Lorenz RD, Smith PH, Lemmon MT, Karkoschka E, Lockwood GW, Caldwell J (1997) Titan's north–south asymmetry from HST and Voyager imaging: comparison with models and ground-based photometry. Icarus 127:173–189
Lorenz RD, Lemmon MT, Simth Ph (1999a) Evidence for clouds on Titan from HST WFPC-2. AAS/Division for Planetary Sciences Meeting 31
Lorenz RD, Lemmon MT, Smith PH, Lockwood GW (1999b) Seasonal change on Titan observed with the hubble space telescope WFPC-2. Icarus 142:391–401
Lorenz RD, Lemmon MT, Smith PH (2000) Variable and constant features on Titan from HST. In: Highlights of planetary exploration from space and from Earth, 24th meeting of the IAU, Joint Discussion 12, August 2000, Manchester, England, 12
Lorenz RD, Young EF, Lemmon MT (2001) Titan's smile and collar: HST observations of seasonal change 1994–2000. Geophys Res Lett 28:4453
Lorenz RD, Smith PH, Lemmon MT (2004) Seasonal change in Titan's haze 1992-2002 from hubble space telescope observations. Geophys Res Lett 31:10702
Lorenz RD, Griffith CA, Lunine JI, McKay CP, Rennò NO (2005) Convective plumes and the scarcity of Titan's clouds. Geophys Res Lett 32:1201
Lorenz RD, Lemmon MT, Smith PH (2006) Seasonal evolution of Titan's dark polar hood: midsummer disappearance observed by the Hubble Space Telescope. Mon Notices R Astron Soc 369(4):1683–1687
Lorenz RD, Zarnecki JC, Towner MC, Leese MR, Ball AJ, Hathi B, Hagermann A, Ghafoor NAL (2007) Descent motions of the Huygens probe as measured by the Surface Science Package (SSP): turbulent evidence for a cloud layer. Planet Space Sci 55:1936–1948. doi:10.1016/j.pss.2007.04.007
Lorenz RD, Stiles BW, Kirk RL, Allison MD, Persi del Marmo P, Iess L, Lunine JI, Ostro SJ, Hensley S (2008a) Titan's rotation reveals an internal ocean and changing zonal winds. Science 319:1649. doi:10.1126/science.1151639
Lorenz RD, West RD, Johnson WTK (2008b) Cassini RADAR constraint on Titan's winter polar precipitation. Icarus 195:812–816. doi:10.1016/j.icarus.2007.12.025

Lunine JI, Atreya SK (2008) The methane cycle on Titan. Nature Geoscience 1(3):159–163. doi:10.1038/ngeo125

Luz D, Hourdin F (2003) Latitudinal transport by barotropic waves in Titan's stratosphere. I. General properties from a horizontal shallow-water model. Icarus 166:328–342

Luz D, Hourdin F, Rannou P, Lebonnois S (2003) Latitudinal transport by barotropic waves in Titan's stratosphere. II. Results from a coupled dynamics-microphysics-photochemistry GCM. Icarus 166:343–358. doi:10.1016/S0019-1035(03)00263-X. http://adsabs.harvard.edu/abs/2003Icar..166..343L. Provided by the SAO/NASA Astrophysics Data System

Luz D et al (2005) Characterization of zonal winds in the stratosphere of Titan with UVES. Icarus 179:497–510. doi:10.1016/j.icarus.2005.07.021

Magain P, Courbin F, Sohy S (1998) Deconvolution with correct sampling. Astrophys J 494:472. doi:10.1086/305187

Matthews K, Ghez AM, Weinberger AJ, Neugebauer G (1996) The first diffraction-limited images from the WM Keck Telescope. Publ Astron Soc Pac 108:615

Mayo LA, Samuelson RE (2005) Condensate clouds in Titan's north polar stratosphere. Icarus 176:316–330. doi:10.1016/j.icarus.2005.01.020

McKay CP, Pollack JB, Courtin R (1989) The thermal structure of Titan's atmosphere. Icarus 80:23–53

Meier R, Smith BA, Owen TC, Terrile RJ (2000) The surface of Titan from NICMOS observations with the Hubble Space Telescope. Icarus 145:462–473

Mitchell JL, Pierrehumbert RT, Frierson DM, Caballero R (2006) The dynamics behind Titan's methane clouds. Proc Natl Acad Sci USA 103:18421–18426

Mitri G, Showman AP, Lunine JI, Lorenz RD (2007) Hydrocarbon lakes on Titan. Icarus 186:385–394. doi:10.1016/j.icarus.2006.09.004

Moreno R, Marten A, Hidayat T (2005) Interferometric measurements of zonal winds on Titan. Astron Astrophys 437:319–328. doi:10.1051/0004-6361:20042117

Negrão A (2007) The characterisation of Titan's lower atmosphere and surface from near-infrared spectra, Ph.D. Thesis

Negrão A, Coustenis A, Lellouch E, Maillard J-P, Rannou P, Schmitt B, McKay CP, Boudon V (2006) Titan's surface albedo variations over a Titan season from near-infrared CFHT/FTS spectra. Planet Space Sci 54:1225–1246. doi:10.1016/j.pss.2006.05.031

Negrão A, Hirtzig M, Coustenis A, Gendron E, Drossart P, Rannou P, Combes M, Boudon V (2007) The 2-μm spectroscopy of Huygens probe landing site on Titan with very large telescope/nasmyth adaptive optics system near-infrared imager and spectrograph. J Geophys Res (Planets) 112:2. doi:10.1029/2005JE002651

Porco CC et al (2005) Imaging of Titan from the Cassini spacecraft. Nature 434:159–168

Pruppacher HR, Klett JD (1978) Microphysics of clouds and precipitation, D. Reidel, Dordrecht, p 714

Rages K, Pollack JB (1983) Vertical distribution of scattering hazes in Titan's upper atmosphere. Icarus 55:50–62

Rannou P, Hourdin F, McKay CP (2002) A wind origin for Titan's haze structure. Nature 418:853–856

Rannou P, McKay CP, Lorenz RD (2003) A model of Titan's haze of fractal aerosols constrained by multiple observations. Planet Space Sci 51:963–976

Rannou P, Hourdin F, McKay CP, Luz D (2004) A coupled dynamics-microphysics model of Titan's atmosphere. Icarus 170:443–462

Rannou P, Lebonnois S, Hourdin F, Luz D (2005) Titan atmosphere database. Adv Space Res 36:2194–2198. doi:10.1016/j.asr.2005.09.041

Rannou P, Montmessin F, Hourdin F, Lebonnois S (2006) The Latitudinal distribution of clouds on Titan. Science 311:201–205. doi:10.1126/science.1118424

Richardson MI, Toigo AD, Newman CE (2007) PlanetWRF: a general purpose, local to global numerical model for planetary atmospheric and climate dynamics. J Geophys Res 112:E09,001. doi:10.1029/2006JE002825

Rodriguez S et al (2009) Cloud activity on Titan: seasonal changes and tidal effects. Nature

Roe HG, de Pater I, Gibbard SG, Macintosh B, Max CE, McKay CP (2000) Near- and mid-infrared resolved imaging of Titan's atmosphere. Bull Am Astron Soc 32:1023

Roe HG, de Pater I, Macintosh BA, Gibbard SG, Max CE, McKay CP (2002a) NOTE: Titan's atmosphere in late southern spring observed with adaptive optics on the WM Keck II 10-meter telescope. Icarus 157:254–258

Roe HG, de Pater I, Macintosh BA, McKay CP (2002b) Titan's clouds from Gemini and Keck adaptive optics imaging. Astrophys J 581:1399–1406
Roe HG, Bouchez AH, Trujillo CA, Schaller EL, Brown ME (2005a) Discovery of temperate latitude clouds on Titan. Astrophys J 618:L49–L52
Roe HG, Brown ME, Schaller EL, Bouchez AH, Trujillo CA (2005b) Geographic control of Titan's mid-latitude clouds. Science 310:477–479. doi:10.1126/science.1116760
Roos-Serote M (2004) The Changing Face of Titan's Haze: Is it all Dynamics? Space Sci Rev 116(1):201–210. doi:10.1007/s11214-005-1956-0. http://www.springerlink.com/content/n2k18248t7303851
Rothman LS et al (2005) The HITRAN 2004 molecular spectroscopic database. J Quant Spectrosc Radiat Transf 96:139–204
Roush TL, Dalton JB (2004) Reflectance spectra of hydrated Titan tholins at cryogenic temperatures and implications for compositional interpretation of red objects in the outer solar system. Icarus 168:158–162. doi:10.1016/j.icarus.2003.11.001
Sagan C, Thompson WR (1982) Production and condensation of organic gases in the atmosphere of Titan. Bull Am Astron Soc 14:714
Sagan C, Thompson WR (1984) Production and condensation of organic gases in the atmosphere of Titan. Icarus 59:133–161
Saint-Pé O, Combes M, Rigaut F, Tomasko M, Fulchignoni M (1993) Demonstration of adaptive optics for resolved imagery of solar system objects—preliminary results on Pallas and Titan. Icarus 105:263
Samuelson RE (1983) Radiative equilibrium model of Titan's atmosphere. Icarus 53:364–387. doi:10.1016/0019-1035(83)90156-2
Samuelson RE, Mayo LA (1997) Steady-state model for methane condensation in Titan's troposphere. Planet Space Sci 45:949–958
Samuelson RE, Mayo LA, Knuckles MA, Khanna RJ (1997a) C_4N_2 ice in Titan's north polar stratosphere. Planet Space Sci 45:941–948
Samuelson RE, Nath NR, Borysow A (1997b) Gaseous abundances and methane supersaturation in Titan's troposphere. Planet Space Sci 45:959–980
Schaller EL, Brown ME, Bouchez AH, Roe HG , Trujillo CA (2004) Continuous monitoring of Titan for large cloud outbursts. In: AAS/Division for Planetary Sciences Meeting Abstracts 36
Schaller EL, Brown ME, Roe HG, Bouchez AH, Trujillo CA (2005) Cloud activity on Titan during the Cassini mission. In: 36th Annual lunar and planetary science conference, p 1989
Schaller EL, Brown ME, Roe HG, Bouchez AH (2006a) A large cloud outburst at Titan's south pole. Icarus 182:224–229. doi:10.1016/j.icarus.2005.12.021
Schaller EL, Brown ME, Roe HG, Bouchez AH, Trujillo CA (2006b) Dissipation of Titan's south polar clouds. Icarus 184:517–523. doi:10.1016/j.icarus.2006.05.025
Sicardy B et al (1990) Probing Titan's atmosphere by stellar occultation. Nature 343:350–353
Sicardy B et al (1999) The Structure of Titan's Stratosphere from the 28 Sgr Occultation. Icarus 142:357–390
Sicardy B et al (2006) The two Titan stellar occultations of 14 November 2003. J Geophys Res (Planets) 111:11. doi:10.1029/2005JE002624
Smith BA et al (1981) Encounter with Saturn—Voyager 1 imaging science results. Science 212:163–191
Smith BA et al (1982) A new look at the Saturn system—the Voyager 2 images. Science 215:504–537
Smith PH, Lemmon MT, Lorenz RD, Sromovsky LA, Caldwell JJ, Allison MD (1996) Titan's surface, revealed by HST imaging. Icarus 119:336–349
Sromovsky LA, Suomi VE, Pollack JB, Krauss RJ, Limaye SS, Owen T, Revercomb HE, Sagan C (1981) Implications of Titan's north–south brightness asymmetry. Nature 292:698–702
Stevenson DJ, Potter BE (1986) Titan's latitudinal temperature distribution and seasonal cycle. Geophys Res Lett 13:93–96. doi:10.1029/GL013i002p00093
Stiles BW et al (2008) Determining Titan's spin state from Cassini radar images. Astron J 135:1669–1680. doi:10.1088/0004-6256/135/5/1669
Stofan ER et al (2007) The lakes of Titan. Nature 445:61–64. doi:10.1038/nature05438
Strobel DF (2006) Gravitational tidal waves in Titan's upper atmosphere. Icarus 182:251–258. doi:10.1016/j.icarus.2005.12.015
Tokano T (2005) Meteorological assessment of the surface temperatures on Titan: constraints on the surface type. Icarus 173:222–242
Tokano T (2008a) Dune-forming winds on Titan and the influence of topography. Icarus 194:243–262. doi:10.1016/j.icarus.2007.10.007

Tokano T (2008b) The dynamics of Titan's troposphere. Philos Trans R Soc A Math Phys Eng Sci 367(1889):633–648. doi:10.1098/rsta.2008.0163

Tokano T, Neubauer FM, Laube M, McKay CP (1999) Seasonal variation of Titan atmospheric structuresimulated by a general circulation model. Planet Space Sci 47:493–520

Tokano T, Ferri F, Colombatti G, Mäkinen T, Fulchignoni M (2006a) Titan's planetary boundary layer structure at the Huygens landing site. J Geophys Res (Planets) 111:8007. doi:10.1029/2006JE002704

Tokano T, McKay CP, Neubauer FM, Atreya SK, Ferri F, Fulchignoni M, Niemann HB (2006b) Methane drizzle on Titan. Nature 442:432–435. doi:10.1038/nature04948

Tomasko MG, Bézard B, Doose L, Engel S, Karkoschka E (2008a) Measurements of methane absorption by the descent imager/spectral radiometer (DISR) during its descent through Titan's atmosphere. Planet Space Sci 56:624–647. doi:10.1016/j.pss.2007.10.009

Tomasko MG, Doose L, Engel S, Dafoe LE, West R, Lemmon M, Karkoschka E, See C (2008b) A model of Titan's aerosols based on measurements made inside the atmosphere. Planet Space Sci 56:669–707. doi:10.1016/j.pss.2007.11.019

Tomasko MG et al (2005) Results from the Descent Imager/Spectral Radiometer (DISR) Instrument on the Huygens probe of Titan. Nature 438:765–778. doi:10.1038/nature04126

Toon OB, McKay CP, Courtin R, Ackerman TP (1988) Methane rain on Titan. Icarus 75:255–284

Turtle EP, Perry JE, McEwen AS, DelGenio AD, Barbara J, West RA, Dawson DD, Porco CC (2009) Cassini imaging of Titan's high-latitude lakes, clouds, and south-polar surface changes. Geophys Res Lett 36:2204. doi:10.1029/2008GL036186

Walterscheid RL, Schubert G (2006) A tidal explanation for the Titan haze layers. Icarus 183:471–478. doi:10.1016/j.icarus.2006.03.001

Young EF, Rannou P, McKay CP, Griffith CA, Noll K (2002) A three-dimensional map of Titan's tropospheric haze distribution based on Hubble Space Telescope imaging. Astrophys J 123:3473–3486

Yung YL (1987) An update of nitrile photochemistry on Titan. Icarus 72:468–472